Macro-scale Computational Analysis Including Porous Media and Free Surface Interaction

For Group Project:

Investigating Stormwater Filters and Bioretention Systems

A Study on the *Hydro Filterra(TM)* System Manufactured by *Hydro-International (UK)*

Individual Report – I2

2nd May 2012

Stephen Pavey
Candidate Number: 023145
Student Number: 570005180

Supervisor: Dr Gavin Tabor

Abstract

Macro-scale Computational Fluid Dynamics on the porous regions of the *Hydro Filterra*$^{(TM)}$ unit, produced by *Hydro International (UK),* is conducted while identifying and extensively validating the modelling approaches used. Both single and multi-phase simulations are achieved, the latter of which utilised a volume of fluid method to identify low-flow regions in the filter media. Focus on the internal media and outflow conditions demonstrates the necessity for uniform meshes to overcome the Rayleigh Taylor instability. These findings were instructive in building a 3D model of the whole system.

Key Words:

Porous-media, *porousSimpleFoam*, *PorousInterFoam,*
multi-phase, Meshing, Rayleigh-Taylor

Acknowledgements:

The following contributions are gratefully recognised:

Dr Gavin Tabor:	For project supervision and invaluable CFD consultation throughout
Daniel Jarman:	As main point of contact at *Hydro International (UK)* and for providing consultation for the CFD elements
Dr Matthew Baker:	For discussion regarding packed bed theory
Augusto Della Torre:	For assistance with using linux in the computer suite in the University of Exeter

Contents

1. Introduction

1.1 Overview

1.1.1 Investigating Stormwater Filters and Bioretention Systems

There are many approaches to dealing with water runoff within urban environments. One innovative design within this field is the *Hydro Filterra*$^{(TM)}$ bioretention system produced by *Hydro International (UK)*. By filtering large particulate matter, a portion of the smaller particulate waste and some chemical pollutants, this design eases pressure on downstream sewerage treatment facilities. To this end, it significantly contributes to the cleaning of surface runoff to meet increasingly strict legislation on water quality.

This group project investigates the flow through the *Hydro Filterra*^{TM} bioretention unit; comprehensively studying the flow behaviour through the porous media by testing soil samples. Parallel to this, analysis of the flow was achieved with the application of micro-CT scans to create computational models. The values from each section are used construct the macro-level Computational Fluid Dynamics (CFD) model, leading to a study of interaction of the unit with the drainage network.

1.1.2 Bioretention Systems

Bioretention Systems hold several layers of engineered porous filter media in a concrete casing which filters out the particulate matter from the flow. As detailed in **figure 1** the surface runoff flows into the system at the kerb inlets. Erosion in the initial mulch layer is prevented by the used of an energy dissipating stone (1). In the main soil region most of the pollutants are filtered out (2) and in the lower gravel layer the water is collected through a perforated outlet pipe as it re-enters the hydrological cycle (3).

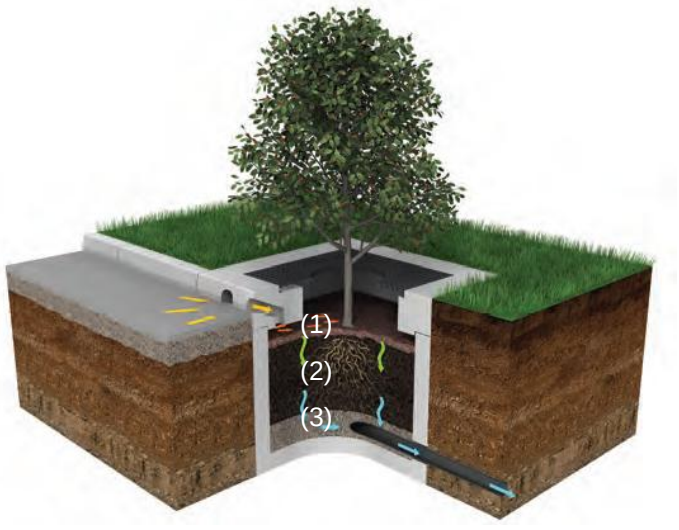

Figure 1. Hydro Filterra$^{(TM)}$ *Bioretention System (ESI 2010)*

In addition, a tree or shrub planted into the media removes chemical pollutants from the flow including the nitrates used for the process of plant growth.

Unlike the energy-intensive downstream water treatment plants, this small-scale filter unit requires no energy from the national grid while filtering a large portion of the chemical and particulate matter at the initial stages. This enhances the urban environment by damping the flow into the drains which can prevent surges in the system.

Difficulties with the design of this system range from the choice of material for both the casing and porous media to the type of plant used in the system. With regard to the filter media selection, the engineered soil been developed in the USA through a system of soil tests which require many months to demonstrate both the flow and chemical removal performance.

Naturally the detailed flow behaviour inside the system is unknown. The casing is designed mainly for good structural performance. It is also specified for operating in an urban environment and to house sufficient media to provide retention rates that allow sufficient time for the unit to remove the pollutants. A method to characterise the drainage inside the unit is required to improve the design of the system. With such a method, new designs could be drafted to yield optimised interstitial flow behaviours which most efficiently use the entire media volume.

1.2 Project Outline

1.2.1 Group Aims

This project aims to comprehensively assess the design of the *Hydro Filterra*$^{(TM)}$ unit. The main deliverables were identified through consultation with *Hydro International (UK).* In particular the need to further develop current computational approaches was highlighted. Since most of the current design work is based around standards and approximations rather than comprehensive numerical approaches, this area of the project holds particular interest to *Hydro International (UK).* Additionally, large scale analysis of the design, from the composition of the filter media to the concrete casing, was identified with particular interest given to the interaction with the wider hydrological cycle. These aims were categorised as four general objectives which were applied to a case study in Barry, South Wales:

1. Develop current CFD approaches to characterise the filter media and verify these results experimentally
2. Develop a three dimensional model of the system including the interaction within the urban environment and outflow from the system including root effects
3. Analyse the current model in terms of the structural design of the casing
4. Consider how the system interacts with the hydrological cycle on a larger scale

The work for the computational approaches and experimental methods was divided between two sub-teams. The individual tasks are shown in **figure 2** which highlights the computational approaches in blue and the civil engineering elements in green. This image outlines how the work completed in this individual section, shown in dark blue, fits with the overall structure of the project. Construction of the 3D model was completed in conjunction with group members responsible for the roots and inlet study.

As can be seen in this **figure 2**, soil sample geometries taken from the case study were captured with a micro-CT scanner and a computer model was constructed at a micro-level. This was then used to create a scaled-up model using Additive Layer Manufacturing (ALM) for experimental testing with Reynolds matched airflow. Additionally the digitised geometry was used to create a system for CFD analysis using Image Based Meshing (IBM) techniques. The model parameters were then used to specify the macro-model constructed from the

investigations outlined in this report. Parallel to this work, the design data and information found from the case study were used to simulate the inlet into the system from the car park and to characterise the flow near the roots of the plant. All three macro-level studies were used to build a preliminary 3D CFD model constructed for the final objective above. The outcomes from the CFD modelling were used to inform the investigation into the interaction with the wider environment.

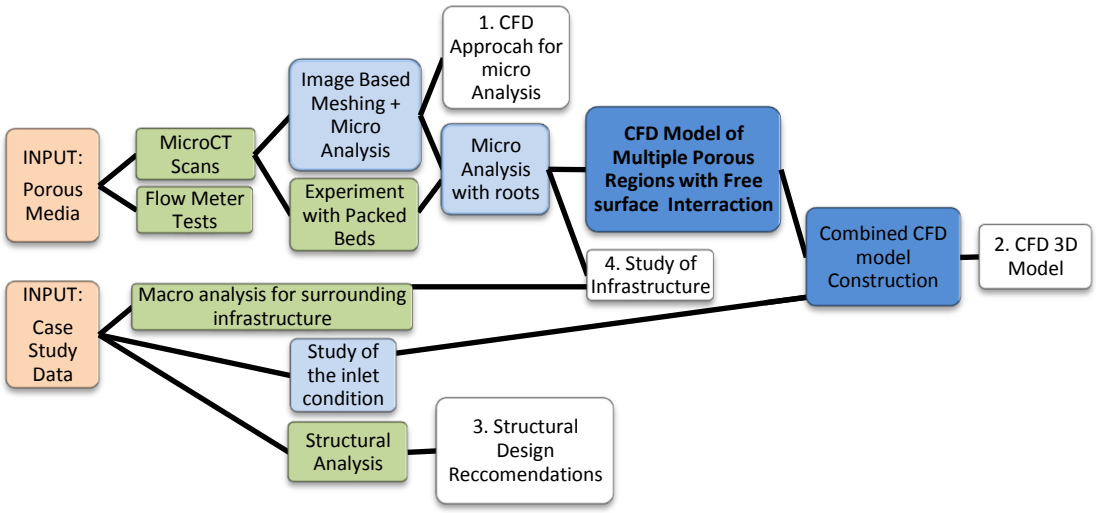

Figure 2. Flow of information within the group project

1.2.2 Individual Section: Modelling Flow in Porous Media at a Macro Level

This individual project investigates the fluid flow through porous media using the CFD code *OpenFOAM*. Using the hydraulic properties provided by the others in the team, an accurate macro-scale model was built for the flow in the porous regions inside the *Hydro Filterra*$^{(TM)}$ bioretention unit utilising the porous media functions coded within *OpenFOAM*. Once verified, these methods were used in the construction of the 3D model.

As described in **section 1.1.2**, the system comprises of two significant porous media regions: soil and gravel. Each of these domains is described by hydraulic properties as determined by the micro-sections of the analysis. This section modelled the fluid with a multi-phase interaction of air and water with appropriate boundary conditions where gravity fed flow and turbulence effects are accounted for as required.

The main geometrical constraint on the model is the outlet which comprises a perforated section of pipe. Since this feature has a significant effect on the flow behaviour in the system, care was taken to assess the best modelling approach to use. This was identified as an area of interest for *Hydro International (UK)*.

This work was then combined with the macro CFD analysis of the surrounding infrastructure and the presence of the roots. This comprises the second task, where in collaboration with the other macro CFD group members, the full 3D flow model was constructed. This work will meet the following objectives and deliverables:

Objectives

1. Identify the steady state porous zone methods available in *OpenFOAM* and verify them with comparison to data in the public domain
2. Complete similar verification for the *interFoam* adaptation to the porous solver
3. Create a CFD model for regions containing engineered media, with multiple filter regions and compare with the experimental data
4. Complete a mesh study for the outlet
5. Compile these macro models with the macro analysis of the inflow and root systems into a final working CFD model of the entire system

Deliverables

1. A working, verified model of a single porous region, using simple inlet / outlet boundary conditions
2. A working, verified model of the same media with multi-phase flow
3. A model used to compare with the experimental results
4. A working CFD model of multi-media multi-phase flow based on the best meshing approach for modelling the outlet pipe
5. A full macro model of the entire system, featuring a number of different flow conditions

Risk Assessment

The work conducted for this individual section was chiefly computational in nature. Therefore the risks associated with this project concern the potential incorrect use of Visual Display Units (VDUs) (Health and Safety Executive 2006) and are identified as repetitive strain injury and eye strain. To mitigate these risks, the monitors used were elevated to the correct level and consideration was given to chair height. Suitable breaks were taken during the more intensive work periods.

Further to this, the risks associated with the site visit in Barry, South Wales were considered by both *Hydro International (UK)* and the project group before the trip was conducted.

Sustainability

The sustainability of this project is of chief importance. The *Hydro Filterra*$^{(TM)}$ unit is designed to reduce loads on downstream treatment plants saving energy. Wider application of such designs and their optimisation provide a sustainable approach to improve water treatment on a wide scale. Further optimisation of this design can be aided by the use of the computational methods outlined in this report.

Professional Responsibility

The work conducted in this group project is governed by a confidentiality agreement between the group members, the University of Exeter and *Hydro International (UK).* As such, the findings included in this report are not to be used to gain commercial advantage and the *Hydro Filterra*$^{(TM)}$ designs remain the intellectual property of *Hydro International (UK).*

2. Literature Review

2.1 Summary from I1

The following summarises investigations using CFD analysis to assess porous media that has been sourced from the public domain. The relevant details of the work and the conclusions reached are briefly outlined in this section based on the literature review completed in the previous submission (Pavey 2011). These resources, with others, are then referenced throughout the theory section of this report.

The most relevant approach which has come to light from this research is a computational method where functions modelling the porous resistance are determined before building the system. This allows adjustment of the porous coefficients to fit the experimental results. A method of a similar nature was followed for this individual project. Statistical approaches were also found but have been omitted in this instance since, to determine the global performance of a porous media, a coarse mesh based on micro analysis was specified for a large region. The statistical integration of small parts over the domain can then be used to characterise the performance for the region on a macro level. As seen below, the majority of the work to date in this area concerns the design of Trickle-Bed Reactors (TBRs) for the petro-chemical industry.

2.1.1 Graded Region Methods

The work completed by the Department of Chemical Engineering at the Indian Institute of Technology, Delhi (Atta, Roy and Nigam 2007) concerns computational analysis of multi-phase flow in a porous region using *FLUNET* 6.2 software. This analysis considered a two dimensional CFD model with the gas phase as primary and the liquid as secondary. The pressure drop was compared to the flow velocity of the liquid and gas and then verified using previous work in both CFD and experimental fields. This showed that CFD can be used to analyse the problem of two-phase flow in porous media in a predictive manner.

The assumptions required to run this analysis consider the porous region to be isotropic, both the turbulence & capillary action to be negligible, the fluids are modelled with no mass interchange and both phases are considered to be incompressible. It was also noted that the relative permeability of the region was specified, since the permeability of a gas in a system is different to that of the fluid. This study also highlighted the potential development of this area, showing that as computer power increases there is greater scope for modelling the porous media more accurately using numerical methods such as CFD.

Other studies have been conducted yielding similar conclusions. The study on two-phase flow distributions (Souadnia and Latifi 2001) utilised similar methods to simulate multi-phase flow in porous media using the same relative permeability model. This required similar boundary conditions and flow properties to define the system. This work focuses on a one dimensional model of the problem outlining slip boundary conditions at the bed walls. This preliminary investigation serves to demonstrate the potential of computational methods in this field and compliments the article outlined above since they share similar flow regimes and boundary conditions.

Additional flow behaviours can be modelled in the same manner by utilising other user-defined functions at the pre-processing stages. Further work from the Department of Chemical Engineering in Delhi (Atta, Roy and Nigam 2007) concerns the maldistribution of fluid in multi-phase flow of TBRs. This investigation demonstrates the effects of inlet conditions on

the distribution on the flow at the outlet of the porous media. To this end, a bed of glass beads was considered as analogous to the TBRs for the analysis. The porosity was simulated with user-defined functions to describe the internal flow. It also outlines the relative permeability method developed by Sáez and Carbonell (Sáez and R.G. Carbonell 1985) shown in **section 3.1.5** for assessing multi-phase flow in porous media. The resulting flow rates inside predefined zones on the outlet were mapped for varying inlet configurations and conclusions were compared to previous work. The maldistribution was based on that first used by others (Petrova, Semkov and Dodev 2003).

Further work completed to model turbulence in TBRs (Lopes and Quinta-Ferreira 2009) used an upwind solver to analyse a packed bed of uniform spheres. Different turbulence models were used in this study to determine which method produced the best correlation to known data, while using computer power efficiently. It was determined that the standard k-ε model for Reynolds Averaged Navier Stokes (RANS) turbulence simulation is the best approach for this area of research. Further work was then completed using this model to analyse the effect of temperature on the flow.

The work completed by Haukur Hafsteinsson (Hafsteinsson 2009) demonstrates the functionality of the *porousSimpleFoam* code in *OpenFOAM*. This report outlines the relevant file structure and operational parameters. Although not a study of the physics behind porous regions, this report is invaluable for making the transition from one or two dimensional analyses of similar systems to construct a representative CFD model in three dimensions.

2.1.2 Other Approaches

There has also been work conducted into packed beds other than TBRs bringing interesting concepts into consideration. For example a study of the mathematics behind the Darcy-Forchheimer equation (Straughan 2010) shows how changes in porosity due to turbulence can be accounted for using this fundamental flow equation for porous media. Both changes in geometry, as the flow slightly redistributes the media, and temperature changes were also accounted for. Similar empirical studies completed in this area (Macini, Mesini and Viola 2011) show how the flow changes with higher pressure gradients than those demonstrated with surface runoff.

Equally a study of packed beds has been achieved through micro-CT investigation into the structure of the porous media (Baker, Young and Tabor 2011) (Baker and Tabor 2010). In particular theoretical, experimental and numerical approaches have been combined (Narsilio, et al. 2009) in a manner which most closely reflects the aims of this project. By analysing porous media from a phenomenological approach; taking Navier Stokes flow equations and Darcy's equation for flow in porous media from first principles, the mathematical basis for the analysis is identified. This is then corroborated by solving the equations numerically before verifying them experimentally using micro-CT scans of the soil. These mathematical derivations underpin the work outlined in this individual report.

A very different approach is to consider the random variations in the flow through the porous media by considering the statistics of the flow behaviour. This stochastic approach (Ma and Zabaras 2011) aimed to pattern the properties of a small section of detailed CFD onto a large area. The integration of the small study in a statistical way allows for changes at the walls to be accounted for from first principles rather than using the built in functions of a given CFD package.

2.2 Further Research

The initial literature review outlined in **section 2.1** highlighted difficulties in specifying multi-phase flow in porous regions. Thus the following further research was conducted in this area to ascertain a framework for the project and identify where this investigation can add value to current understanding.

On the micro-scale, investigations have been conducted into tracking multi-phase flow through the pores of soils. In particular, work completed by the University of Texas (Prodanovic and Bryant 2006) modelled the flow for a static sample of spheres with a fixed surface tension and pressure. This approach indicates the non-trivial nature of creating geometry at this scale and tracks non-reversible behaviour, in particular through the interaction of meniscuses. Although this micro-level work does not directly mirror the work proposed in this investigation, it is a good example of how a Volume Of Fluid (VOF) approach can be applied to porous regions.

Work has also been completed regarding the flow of water and oil in systems involving a heterogeneous porous medium (Berre, Lien and Mannseth 2009). This is an example of a two-phase seepage problem where a level-set VOF function is used to estimate the flow patterns. Meticulous refinement methods were used to iteratively build up the domain from a coarse representation to a fine mesh which accurately represents the changes in porosity across the region. This journal also touches on this inherent instability of this approach which arises from the large degree of freedom in the calculations around the free surface, particularly across changes in porosity, which requires such a tentative meshing approach.

Further work with a miscible set of fluids, water and brine, provides an interesting demonstration of seepage in saturated porous media (Johannsen, et al. 2006). In this case investigation of saltwater-freshwater 'fingering' was conducted using a similar level-set approach, although in this case the field variable changed over a greater range to allow for mixing of the fluids. In this case the Rayleigh-Taylor instability was identified as a significant issue arising as the downward flow of the denser phase induced an upward flow of the lighter phase. Although similar trends in flow were achieved with non-invasive experiments on an equivalent experimental system, the inevitable inaccuracies in the model and extremely non-linear behaviour of the system prevented like-for-like reproduction of results. This report suggests that the instabilities are linked in greater part to the underlying mathematics and to a lesser degree from the system geometry. It is noted however that refinement of the geometry allowed the model to be solved in some cases.

The most thorough investigation into varying flow phenomena for porous zones regards the change in porosity with saturation (Braun, Helmig and Manthey 2006). Taking assumptions that negate capillary action, this investigation used micro-analysis of saturation levels and the associated micro field porosities were renormalised over the whole region giving rise to a case-specific relative permeability model. The conclusions reached in this investigation demonstrate the importance of saturation on the porosity and the significant complexity involved in identifying these effects.

2.2.1 Articles for Validation

Two further journals were invaluable for validating the models in this project. The former drafted report, supplied by Dr Gavin Tabor (Tabor, et al. 2004), demonstrates how a porous region can be defined within the CFD code, *FLUENT*. This compared the CFD simulations to experimental work on flow behind windbreaks, which was completed by the University of Pohang in South Korea (Lee and Kim 1999) where Particle Tracking Velocimetry (PTV) was

used to track the flow behaviour in the wake of the fence. Of greatest interest is how the pressure drop across the region was specified with the Forchheimer augmentation of the Darcy relationship as outlined in **section 3.3.2**.

The physical relationship for this definition is described and the barrier coefficients outlined based on physical properties of the region such as the void fraction. It was noted that some coefficients were selected to fit the experimental data and were not based on porous geometry or flow properties. However, the trends yielded from the code demonstrate the potential of this model. There is scope from this work to determine an alternative method for defining the porous region based only on physical properties and for validating the equivalent porous region solver in *OpenFOAM*.

Secondly, the porous region techniques were developed by adopting multi-phase approaches to the flow. The work in later stages of this project concerned the addition of the VOF method *porousInterFoam*. This solver uses the graded free-surface techniques employed by the utility *interFoam* while incorporating a porous sink term to the Navier Stokes equations. A study in collaboration between universities in Madrid and Morocco (Herreros, Mabssout and Pastor 2006) completes a numerical study, tracking the free surface through porous media with level set approach for two immiscible fluids in a manner similar to *interFoam*. These computational methods serve to provide a good validation for the *porousInterFoam* model considered in **section 4.4**. Further to this, the report demonstrates the value of using free surface methods for CFD models of seepage in porous domains.

2.2.2 Conclusion

It can be concluded from this research that although many methods for modelling the flow through porous media have been established, it is the combination of these methods where there is significant room for development. Particularly the investigation of multi-phase flow through a homogeneous porous region in three dimensions is a significant challenge when taking into account the nature of relative porosity, dependence on saturation and the numerical instabilities associated with constructing such models.

Additionally there were no research papers found demonstrating this type of analysis on the open source CFD software *OpenFOAM*. Therefore the initial value of this individual section of the project will be in establishing a macro-scale model for the flow through the *Hydro Filterra*$^{(TM)}$ porous media, and in demonstrating the capability of *OpenFOAM* in modelling this type of problem.

To this end, the structure of this project investigates the program sequentially, aiming to use of the full porous media functionality within the *OpenFOAM* code. Firstly a method to establish the porosity of the region based on physical properties of the soil was required. The validation of the steady state *porousSimpleFoam* algorithm was conducted and this was further validated with respect to the experimental work completed by others in this project.

Building on this foundational work, the VOF method, *porousInterFoam* forms a good avenue for evaluating the multi-phase flow in porous media. Validation for this solver was required to verify later conclusions. Multiple avenues for generating the model geometry were investigated in order to minimise model instabilities. This work was completed for unsaturated media with porosity defined in the same way as in the steady state case.

Further investigations into the effects of relative permeability or saturation-dependant porosity were identified from this literature review as extensions for this project. However, it is noted

that due to the low velocities and long time-scales involved with bioretention, it can be argued that fixed porosity modes reasonably replicate the flow behaviour within the porous zones. Given the achievable degree of accuracy when using VOF methods, saturated or unsaturated cases can be considered to sufficiently represent the flow patterns to inform design changes. Therefore VOF of unsaturated models were investigated with a view to increasing the model complexity to account for relative permeability at a later date.

3. Theoretical basis for CFD calculations within Porous Media

The physical and mathematical basis for the work completed for this report is outlined in this section. Care is taken to identify appropriate bases for defining flow based on Darcy's law and subsequent adaptations on the same. Turbulent and wall effects are also considered although they are shown to have little effect at this scale due to the low flow rates in the *Hydro Filterra*$^{(TM)}$ unit. Other conditions are also described to explain why they are assumed to be negligible such as capillary action, seepage and relative permeability although further study is recommended to confirm this. The content of **sections 3.1** through **3.4** is edited from the preliminary report for this work (Pavey 2011) and respects minor changes in project direction.

3.1 Darcy Equation for flow in Porous Media

3.1.1 Darcy's equation

The most basic mathematical representation of a porous region is the volume fraction. This value ε, represents the volume of free space over the total volume as shown in **equation 1**.

$$\varepsilon = \frac{V_f}{V_t}$$

Eqn 1.

However, this value is too simplistic to adequately scale a pressure drop across the region. The flow through the media is affected by the volume of particle surfaces, the tortuosity of paths through the media, the effects of dead end pathways and the surface quality of the filter media as well as fluid effects such as surface tension and viscosity. Thus it is difficult to construct a model for porous resistance to the flow based on geometry alone in this way.

Henry Darcy's equation relates the flow rate of a fluid in a porous region Q, to its cross sectional area, A, change in piezometric head between two points in the flow, h_1 & h_2, and the length in the direction of the flow L, as shown in **equation 2** (Bear 1972). This work, completed in 1856, accounts for the resistance to the flow based on the porous resistance as K, the hydraulic conductivity. Since it is an experimentally based method, this coefficient accounts for all the factors causing resistance to the flow mentioned above.

$$Q = KA(h_1 - h_2)/L$$

Eqn 2.

It is useful to define the hydraulic gradient at this point as the quotient of the piezometric head over the length as shown in **equation 3.**

$$J = (h_1 - h_2)/L$$

Eqn 3.

A more rigorous method considers the total driving force for the flow through the region as the difference in energy (including kinetic energy), pressure and turbulence. However for flow at atmospheric pressure it is generally considered that the kinetic energy and additional pressures are negligible in comparison to the piezometric head.

In the case of a vertical column, fluid will flow from a region of high pressure caused by the resistance of the media and weight of the fluid, to low pressure as it filters through the soil. Additional pressure driving flow is more often considered for lateral filtration. Lateral flow may occur in the lower sections of the *Hydro Filterra*$^{(TM)}$ unit where the flow tends toward the outlet, however this is not considered in this analysis. Turbulence and rotational flow effects are ignored since they can be considered to be negligible with respect to the piezometric head, especially for laminar flows which are found in this case. The piezometric head at a point can be described by the elevation head z, pressure P, over the density ρ and acceleration due to gravity g, as shown in **equation 4** (Corapcioglu 1996, 195).

$$h = z + \frac{P}{\rho g}$$

Eqn 4

Thus the hydraulic gradient described in **equation 3** is understood as a function of the energy difference in the fluid based on the head alone.

3.1.2 Hydraulic Conductivity

The coefficient K, in **equation 2** represents the hydraulic conductivity of the system. For media which has isotropic geometry it can be considered as the specific discharge per unit hydraulic gradient. This value is often determined experimentally for soil applications, although there are approximate derivations for this value from porous geometries identified in **section 3.2.3**. However, it is not simply a function of media properties but is specific to the fluid considered as well as the porous geometry. It can be calculated using **equation 5** (Bear 1972) which shows hydraulic conductivity was a function of the intrinsic permeability k, the density of the fluid ρ and the acceleration due to gravity g and the dynamic viscosity μ.

$$K = \frac{k\rho g}{\mu}$$

Eqn 5.

The intrinsic permeability is a property of porous media which can have complex geometry. Therefore, it is difficult to derive from first principles. Since fluid properties are required to calculate the hydraulic conductivity, the relative porosity discussed in **section 3.1.5** may be required for multi-phase applications. Intrinsic permeability, k, is usually determined experimentally using the relationship shown as **equation 6** where the length of the experimental bed L and the change in the head of the source water h_o to h, are measured after time t. (Maitra, Ghose and Maitra 2008, 136)

$$k = \frac{L}{t} ln \frac{h_o}{h}$$

Eqn 6.

The actual permeability k_a also depends on the soil saturation S as shown in **equation 7** (Crolet 2000).

$$\boldsymbol{k_a = k\varepsilon exp(\beta S)}$$

Eqn 7.

Here the values for the permeability, are shown as vectors to account for the anisotropy inherent to many soils and clays. The term ε represents the porosity defined in **equation 1**. βS is a constant multiplied by the saturation; the volume of water to volume of free space. These relationships are most useful for direct calculation when using beds with known particle volumes. This is possible for TBRs based on spherical elements but can only be estimated engineered filter media.

3.1.3 Turbulence and Darcy's Equation

The fundamental description of Darcy's law as described above is only valid for laminar flow conditions. The Reynolds number for flow in packed beds is given as **equation 8** (Bear 1972, 125) which is quantified by the flow velocity u, the average grain diameter as approximated in this work as the median grain diameter from sieve tests d_{50}, and the kinematic viscosity v.

$$R_{dp} = \frac{ud_{50}}{v}$$

Eqn 8.

The flow regimes across a range of values for this Reynolds number as described in *Fundamentals of Water Treatment Unit Processes* are shown below in **table 1**. With comparison to the conclusions reached in the University of Exeter.

Table 1 Critical Reynolds Numbers for Porous Media (Hendricks 2011, 821) (Baker, Young and Tabor 2011)

Regime	Reynolds Number	
	Hendricks	Baker et al.
Laminar	<1	<10
Inertial	1-100	
Transitional	100-800	10-300
Turbulent	>800	>300

As with all critical Reynolds numbers, judgement is required to identify when the flow has transitioned from one region to another. Taking into account the differences between sources, a liberal estimate for the laminar region will be used in this report (Bear 1972). Therefore the laminar region is considered for Reynolds numbers less than 10 although some sources suggest a value of <1 to be more appropriate. It is noted that a filtration bed is not a high velocity flow system and it is only the forced flow conditions of a storm surge that could lead to turbulent effects in the filter media and are therefore omitted from the analysis.

Rainfall data from the region indicate the bioretention units have to cope with a worst case inlet velocity of 0.00035 m/s which is used for this study. The laminar flow in this case is demonstrated by rearranging **equation 8** to solve for the particle diameter when flow is on the limit of the laminar region. Using the kinematic viscosity of water of 1.307×10^{-6}, (Engineering Toolbox 2010) the maximum particle diameter was found as 37×10^{-2} m which is far greater than the value of 0.23 mm for the tested filter media. Thus it is thus reasonable to assume all cases to be laminar. This is mirrors the conclusions from the CFD work completed at a micro level for this project (Begley 2012) and other work (Baker, Young and Tabor 2011).

3.1.4 Anisotropic Porosity

The flow through a porous media is very unlikely to be uniform unless very special cases are considered. Even with relatively simple geometries such as packed beds of cylinders seen in previous work (Baker and Tabor 2010), the system cannot be fully isotropic since the random packing of the bed will yield different flow properties in different directions. Indeed the only case where an isotropic bed can be constructed is for media made from packed spheres as shown in **figure 3**. This is a TBR where the catalysts are manufactured to provide uniform results over a given length.

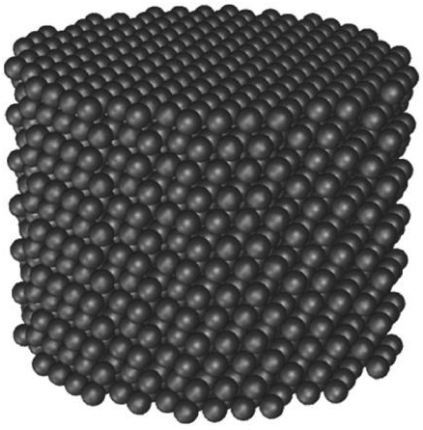

Figure 3. Isotropic packing of catalyst beads (Lopes and Quinta-Ferreira 2009)

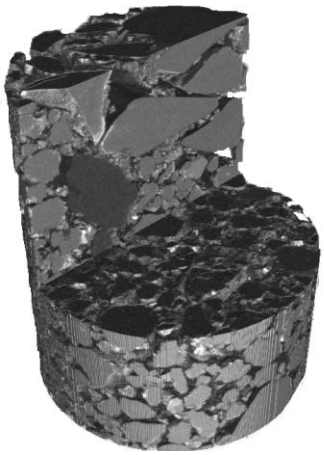

Figure 4. Anisotropic particles from micro-CT data and ScanIP IBM (Please 2012)

However beds made from more random particle sizes, albeit between ranges of sizes for a specific engineered filter media, will exhibit a high level of anisotropy. This is clearly seen in **figure 4** which is a three dimensional model of gravel built for this project. Here the heterogeneity of the region is clearly shown with comparison to the uniform packing of the trickle bed reactor in **figure 3**. The hydraulic conductivity and the driving energy of the fluid (equivalent to piezometric head as example above) vary across each dimension of the region.

However, as with the assumptions made by Atta (Atta, Roy and Nigam 2007), the vertically draining flow can be modelled with an isotropic porous zone since only the flow draining vertically through the media is considered. Although there will be anisotropic geometry which would cause interesting fluctuations in the flow behaviour as drainage circumvents areas of high resistance, this would manifest as random variations about the average flow in the media and a study of this nature would require a more statistical approach.

3.1.5 Relative Porosity

One further approach found in previous work (Atta, Roy and Nigam 2007) avoids using free surface methods. The hydraulic conductivity, K is augmented by the equivalent values for the gas, in order to account for the properties of both fluids in the system. This is most useful for foams where both fluids are largely intermixed as opposed to inflows of relatively separate two-phase systems like the initial flow into the *Hydro Filterra*$^{(TM)}$ unit. The relevant equations are shown below as **equation 9.**

$$\frac{F_\alpha}{\gamma_\alpha} = \frac{1}{k_\alpha}\left[A\frac{Re_\alpha}{Ga_\alpha} + B\frac{Re_\alpha^2}{Ga_\alpha}\right]\rho_\alpha g \quad , \quad Re_\alpha = \frac{u_\alpha \rho_\alpha d_e}{\mu_\alpha(1-\gamma)} \quad , \quad Ga_\alpha = \frac{\rho_\alpha^2 d_e^3 \gamma^3}{\mu_\alpha^3(1-\varepsilon)^3}$$

Eqn 9.

The drag force per unit volume F_α, is given as a function of the holdup γ, intrinsic permeability k, the equivalent particle diameter d_e, the viscosity μ Reynolds number Re_α, Galileo number $Ga_\alpha$and density P_α of the α phase. The Reynolds and Galileo numbers are also defined in **equation 9**. This relationship can be used to find a modified value for k based on the other parameters such as holdup which is caused by any difference in flow speeds between the two phases. As an extension to this study it may be instructive to run the CFD algorithms for both methods to highlight which approach is more appropriate in this case.

3.2 Adapting the Navier Stokes Equation

3.2.1 Navier Stokes equations

The lagrangian Navier-Stokes equation for fluid flow is shown in **equation 10** (Hafsteinsson 2009). Broadly speaking, the Navier Stokes equates the change in momentum of the flow on the LHS to the forces on the flow shown on the RHS and is the fundamental relationship which is evaluated across each element in the domain for CFD applications.

$$\frac{\partial}{\partial t}(\gamma\rho u_i) + \frac{\partial}{\partial x_j}(\rho u_i) = -\frac{\partial P}{\partial x_i} + \mu\frac{\partial \tau_{ij}}{\partial x_j} + S_i$$

Eqn 10.

The value γ is equivalent to porosity, determining the inflow at the initial term. An impermeable material would have the value of 0. The sink term, S_i is equivalent to the resistive force from the porous media with a given level fluid.

3.2.2 Forchheimer's adaptation of Darcy's law

Forchheimer's adaptation of Darcy's law was found to incorporate two momentum losses. This is given by the relationship in **equation 11** which has units similar to the LHS of the Navier Stokes equation, representing a change in momentum.

$$S_i = -\left(\mu D + \frac{1}{2}\rho|u_{jj}|F\right)u_i$$

Eqn 11. Darcy Forchheimer's equation for Navier Stokes for a homogenous region (Hafsteinsson 2009)

The variables of viscosity and density are augmented by the scalar coefficients D and F applied to the flow in order to enable variation for modelling turbulence. The two terms define pressure drop in the fluid due to the particulate obstructions. These values can be found both empirically and through micro CFD analysis and can be input directly into the *OpenFOAM* model in a file named *porousZones*.

The second term (F) accounts for the inertial losses and the former (D) for the viscous losses. (ANSYS Inc. 2009) It is noted that this approach allows the physical nature of porous zones to be accounted for according to the method described in **section 3.2.3**.

3.2.3 Modelling the pressure drop – Ergun and Blake-Kozeny

The Darcy-Forchheimer equation is not the only relationship which is used to represent the pressure drop across a porous medium. A similar approach was found through investigating the workings of the *FLUENT* code (ANSYS Inc. 2009). These relationships are defined for the Ergun equation and are shown below as **equations 12** and **13** where d_p represents the average

particle diameter and u_∞, denotes the free stream velocity. The Ergun equation is a similar model to the Darcy Forchheimer adaptation outlined above. This relates the pressure drop over length to the physical properties of the media and the viscosity, as shown in **equation 14**.

$$D = \frac{150\ (1-\varepsilon)^2}{d_p \varepsilon^3}$$

Eqn 12

$$F = \frac{3.5(1-\varepsilon)}{d_p \varepsilon^2}$$

Eqn 13

$$\frac{|\Delta P|}{L} = \frac{150\mu(1-\varepsilon)^2}{{d_p}^2 \varepsilon^3} u_\infty + \frac{1.75\rho(1-\varepsilon)}{d_p \varepsilon^3} {u_\infty}^2$$

Eqn 14

The first term in the Ergun equation is known as the Blake-Kozeny relationship for laminar flow. The Ergun relationship follows the same format as the Forchheimer adaptation.

As highlighted from the work at the University of Exeter (Tabor, et al. 2004), it is a significant challenge to find a method for defining the porous regions from physical quantities. Therefore these relationships were used to provide initial coefficients which were then modified with respect to the ALM experimental flow data.

3.3 Other Phenomena

3.3.1 Wall distribution effects on porosity

In this project the micro-scale CFD analysis will investigate small samples of the filter medium which are limited by the maximum sample size of the micro-CT scanner. The scans of the filter medium are meshed and CFD is then conducted to determine the pressure drop.

This approach requires the consideration of the difference between a packed bed and packed columns. Packed beds are defined here as large systems where wall effects do not significantly affect the flow in the main body of the region. Conversely packed columns are defined as systems where wall effects are dominant due to the small geometry. The wall of the sample tube limits the location of the larger particles to towards the centre of the column so only significantly smaller than average particles may fit in these spaces or they are left void. An accurate model of a packed bed would require the truncation of particles at the wall; however this is not possible in permeameter tests, especially with the coarser samples. However the meshed models conducted by A. Begley were truncated to allow for this effect which was then carried forward into the ALM experiments. The packing effects at the wall should not be significant on the 1:1 scale CFD models of the bioretention unit and this effect is ignored in this section of the project.

3.3.2 Capillary Action

On a molecular level, adhesive forces act between a fluid and solid present in the flow. At the free surface of a fluid this causes a meniscus as the adhered liquid sits above the free surface level. The adhered fluid is connected to the body of the liquid through surface tension between the fluid molecules. Where the adhesive forces are large enough to compete with the forces in

tension in the fluid, the surface can rise up the solid face. This is known as capillary action. This upward flow is only stopped when the adhesive and cohesive forces are brought into equilibrium by the effect of gravity on a greater mass of water raised above the normal surface level.

This effect is barely noticeable in large containers but in small tubes, masses of fibres or porous media this effect can be significant. However since the flow is seeping slowly though the porous media, the gas-liquid interaction is low and the effect can be ignored as seen in previous work (Atta, Roy and Nigam 2007).

4. Computational Investigation

4.1 Introduction

4.1.1 Plan for study of Porous Media in *OpenFOAM*

As stated in **section 2.2.2** the computational investigation conducted for this report progresses through the basics CFD of porous media using *OpenFOAM* by validating the *porousSimpleFoam* utility. This method was then used to construct a model of the soil regions in the *Hydro Filterra*$^{(TM)}$ unit to be compared to the experimental and micro CFD work completed by others. In particular this involved identifying a method for specifying the filtration media based on geometric data and fitting this to the experimental results as described in **section 3.2.2**.

The work progressed to validating the *porousInterFoam* solver and constructing relevant geometry for multi-phase tests. In this instance a significant volume of the work concerned identifying the preferred mesh generation technique to minimise geometrically induced instabilities in the calculation. This work is expected to be particularly interesting to *Hydro International (UK)* as a subject-specific study on meshing techniques which could be used to inform the purchase of alternative software licences.

The work conducted on the *porousInterFoam* simulations considered a saturated inflow condition to demonstrate the functionality of the solver. The particular inflow conditions at the inlet were studied in greater detail by J. Tarrant while the outlet conditions are considered here.

4.1.2 Approach to validation

In the absence of non-invasive experimental data on the *Hydro Filterra*$^{(TM)}$ unit such as Particle Image Velocimetry (PIV) (Johannsen, et al. 2006) it is through demonstrating the quality of the solver against arbitrary data that a reasonable level of confidence can be placed in the results yielded from later models.

Additionally, due to the comparative accuracy of single-phase approaches highlighted in the literature review, the comparison to work of other group members was made with this approach. The instabilities associated with the *porousInterFoam* solver lead to it being validated with broad agreement with flow patterns rather than direct numerical comparison. As such, design suggestions later in the investigation are recommended tentatively.

4.2 Initial Models

4.2.1 *PorousSimpleFOAM* program outline

The initial models were constructed on the steady-state solver p*orousSimpleFoam* which is an adaptation to the basic algorithm *simpleFoam.* In this case the Navier Stokes equations which are solved over each cell include the sink term as outlined in **section 3.2.2**.

The software *OpenFOAM 2.1.0,* used in this project, contains multiple codes for use in a range of flow scenarios. It is designed to run on the *Linux* operating system giving the user full control of the simulation. The program is installed with a range of tutorials which are used to construct the CFD models for use with each solver. In this case the *angledDuct* tutorial case files formed a basis for the initial models.

The file structure of this case is shown in **figure 5.**

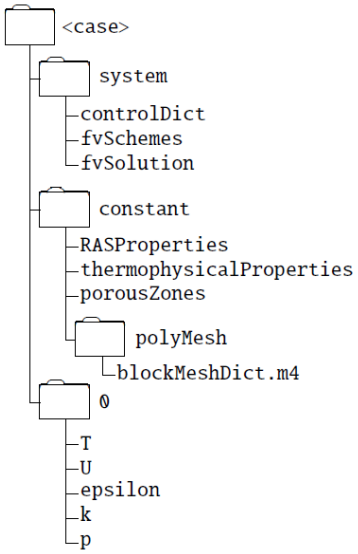

Figure 5. File Structure for angledDuct (Hafsteinsson, Porous Media in OpenFOAM 2009)

The system folder contains the definitions for the calculation, identifying time steps and iterations in the *controlDict*, the discretisation methods in *fvSchemes* and the methods to solve the matrices in *fvSolution*. The *constant* folder includes the turbulence model and the *blockMeshDict.m4* specifies the region and mesh. The *0* folder specifies the initial conditions, including the inlet velocity. The *porousZones* specifies the hydraulic conductivity and is of great interest for this report. A section of this file is shown in **figure 6**.

```
2
(
    soil
    {
        coordinateSystem
        {
            e1   (0 0 1); //assures e1 is in direction of resistance force (z+ve)to resist flow
            e2   (1 0 0);// arbitrarily assigning e2 vector, as x=1 y will be generated by RHR
        }
        Darcy
        {
            d   d [0 -2 0 0 0 0 0] ( 5e6 5e6 5e6); //same in all 3 directions - isotropic
            f   f [0 -1 0 0 0 0 0] (0 0 0);
        }
    }
)
(
    gravel
    {
        coordinateSystem
        {
            e1   (0 0 1);  //same vector as above
            e2   (1 0 0);
        }

        Darcy
        {
            d   d [0 -2 0 0 0 0 0] (7e7 7e7 7e7); //additional resistance to flow wrt above.
            f   f [0 -1 0 0 0 0 0] (0 0 0);
```

Figure 6 Extract from the PorousZones file

In this file the co-ordinate system defines the direction of the hydraulic resistance in the media. Arbitrary D values are selected similar to those found in the tutorial case for the regions respecting the relative significance of the D term in the Forchheimer equation. The names 'soil' or 'gravel' are established in the block section of the *blockMeshDict* where the separate regions of the model are categorised for these simple cases

The notes sections, blocked from being read by the code by the '//' entries have been added for the sake of clarity between group members and indicate the understanding of the functionality of this solver. The vectors above specify a unique co-ordinate system with respect to the global system for each case, and are set to ensure the primary resistance is a vector facing opposite to the inlet, in accordance with the vertical axis of the model. The number at the start of the file indicates that there are two entries and must be added for the solver to read the 'gravel' information.

4.2.2 Demonstration of the Porous Pressure Drop

The *angledDuct* case was modified to simulate the geometry of the *Hydro Filterra*$^{(TM)}$ unit. A 1.2 x 1.2 m drainage section was modelled in a 1.8 m high box suiting an estimate for the size of the unit based on the sizing guides (Hydro International 2010). Porous zones with the same characteristics shown above were specified with blocks between the heights of 1 m and 1.5 m and between 0.4 m and 1 m, with a free region for fluid flow as inlet and outlet space. The steady state algorithm *porousSimpleFoam* was executed. The contour plot and the pressure drop plotted over a line vertically up the centre of the domain are shown as **figure 7**.

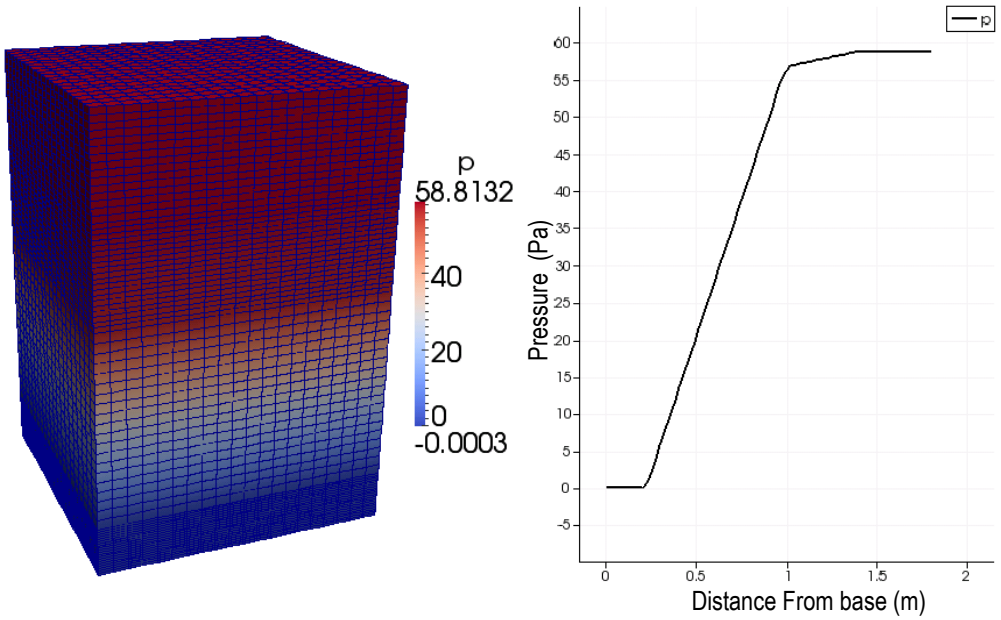

Figure 7. Demonstrating the functionality of the porous region

Not only does this graph clearly show the uniform pressure gradient as expected from the laminar Darcy condition but the values shown on the graph can be used to verify the model's adherence to the Darcy Forchheimer equation. The far steeper gradient in pressure shown in the initial section of the curve mirrors the arbitrarily specified higher resistance value of D applied to the 'gravel' region in this case.

The hydraulic gradient in **equation 2** can be substituted for the S_i term shown in **equation 11**. In this case where the inertial force is set to zero for simplicity, the hydraulic gradient is simply equal to the product of the flow speed, viscosity and scalar D. Ignoring the inertial component of the loss is reasonable since the flows experienced are likely to be within the laminar region.

Since *OpenFOAM* calculates values in incompressible simulations per unit density the kinematic viscosity ν, was used for dimensional consistency. The retarding force is represented as P_{OF}A to signify pressure per unit density multiplied by the cross sectional area.

$$P_{OF}A = vu(D_1 + D_2)$$

$$D = \frac{P_{OF}A}{vu} = \frac{55 \times 1.2^2}{1.5 \times 10^{-5} \times 0.001} = 7 \times 10^7 \qquad (1sf)$$

$$D = \frac{P_{OF}A}{vu} = \frac{(58 - 55) \times 1.2^2}{1.5 \times 10^{-5} \times 0.001} = 5 \times 10^6 \qquad (1sf)$$

This calculation yields the expected values for D as specified in *porousZones* demonstrating that the porous solver behaves as expected.

4.3 *PorousSimpleFOAM* Validation

4.3.1 Research basis

In order to assess the effectiveness of *OpenFOAM* for modelling the flow behaviour in porous regions, a systematic approach to validation was required. As briefly outlined in **section 2.2.2** the work by Lee and Kim used particle imaging techniques to characterise the flow behind porous fences.

The water tank tests in the study used simulated the atmospheric boundary layer by matching the Reynolds numbers for comparable flow conditions. The fence was constructed from a plate built using CNC manufacturing, with a matrix of holes which allowed fluid to pass through while giving uniform geometry to allow for a good estimation of the theoretical porosity. The flow was characterised using PTV methods which uses polystyrene particles in the flow to scatter light from a 150 W halogen lamp. Flow patterns were picked up by a CCD camera through a cylindrical lens and velocity profiles were established using a time interval of 1/30 s between frame captures (Lee and Kim 1999).

4.3.2 Building the computational model

In order to replicate the experimental conditions for validation, the geometry was constructed in *blockMesh* as an adaptation of the *damBreak* tutorial which encompasses the basic block construction for a flow over a dam. The block definitions were amended to define the porous region in the dam location. The system was simulated as a two dimensional model, by setting both front and back patches to 'empty'. The wall conditions were set as zero velocity, fixed pressure gradient wall conditions within the */0* directory.

The Reynolds number was calculated with respect to the height of the porous fence h which was 1 m tall. In order to match the Reynolds number using water the velocity of 3.1 m/s was required.

$$Re = \frac{Uh}{v}$$

$$20900 = \frac{U \times 0.1}{1.5 \times 10^{-5}} \quad => \quad U = 3.1\, m/s$$

The system was built with the k-ε turbulence model following indications from studies that this is the best approach (Lopes and Quinta-Ferreira 2009). This was also chosen for its relative stability within free stream flows (CFD Online 2010). The relationship used to estimate the

value for turbulent energy *k* is given by **equation 15** and the formula for an estimate of the dissipation of turbulence, ε using the estimate of *k* is given as **equation 16** (Tabor, Tutorial Sheet 1 2012).

$$k = \frac{2}{3}(U_{ref}T_i)^2$$

Eqn 15.

$$\epsilon = C_\mu^{\frac{3}{4}} \frac{k^{3/2}}{0.07l}$$

Eqn 16.

U_{ref} is a given velocity, in this case the inlet velocity of 3.1 ms^{-1}, and the turbulent intensity, T_i is given as a percentage. The length scale, l is the height at the inlet in this case and the value C_μ is a coefficient with the value of 0.09, taken from the *k*-ε turbulence model.

The boundary condition, *kqRWallFunction* within the */0, k* file is an initial value for the turbulent energy based on this estimate. The turbulence intensity is set to between 5 and 20% for a high turbulence case, between 1 and 5% for medium turbulence cases and much less than 1% for low turbulence cases as in this case (CFD Online 2012).

Thus the *k* and ε values were calculated as shown by **equations 17** and **18**.

$$k = \frac{2}{3}(3.1 \times 0.1)^2 = 0.0641\ m^2s^{-2} \text{ (3sf)}$$

Eqn 17.

$$\epsilon = (0.09)^{\frac{3}{4}} \times \frac{(0.0641)^{3/2}}{0.07 \times 0.2} = 0.190\ m^2s^{-3} \text{ (3sf)}$$

Eqn 18.

For an accurate simulation these are input into all the uniform values for *kqRWallFunction* in *0/k* and all values inside *0/epsilon* files respectively.

In order to specify the porosity of the region the method used by the *FLUENT* study (Tabor, et al. 2004) was mirrored for consistency. This method is also corroborated by the *ANSYS* manual for specifying porous fences (Tabor, et al. 2004) (ANSYS Inc. 2009). The relationships are shown below as **equations 19** and **20** which were input in the porous zones file.

$$D = \frac{3\rho}{8\mu}\left(\frac{1}{\beta^2} - 1\right)$$

Eqn 19

$$C2\ (F) = \frac{1}{C^2 d}\left(\left(\frac{A_p}{A_f}\right)^2 - 1\right)$$

Eqn 20

The void volume fraction, β is the same as the ratio of pore to total fence area in the drilled fence $\frac{A_p}{A_f}$. The fence thickness is d, and the coefficient C is input as 0.98 as in the journal in order to ensure a good fit to the experimental data.

4.3.3 Results and discussion

The system was solved for a range of porosities to demonstrate the degree of variation in flow patterns. The velocity plot of the resultant simulation is shown in **figure 8** for the 40% porosity case with the location and height of the porous fences highlighted. This, compared to the PTV shows some difference to the trends.

Initially the recirculation demonstrated in the experimental data is not accurately modelled by this case, although this is not surprising since the number of mesh elements is not fine enough for Direct Numerical Simulation (DNS) which also requires transient effects to be considered. However, the increased velocity and turbulent region directly above the fence mirrors the flow behaviour well. The flow can be seen to be translating through the fence as indicated in **figure 8.** Behind the fence the flow is significantly retarded, with limited turbulence as in the experimental results.

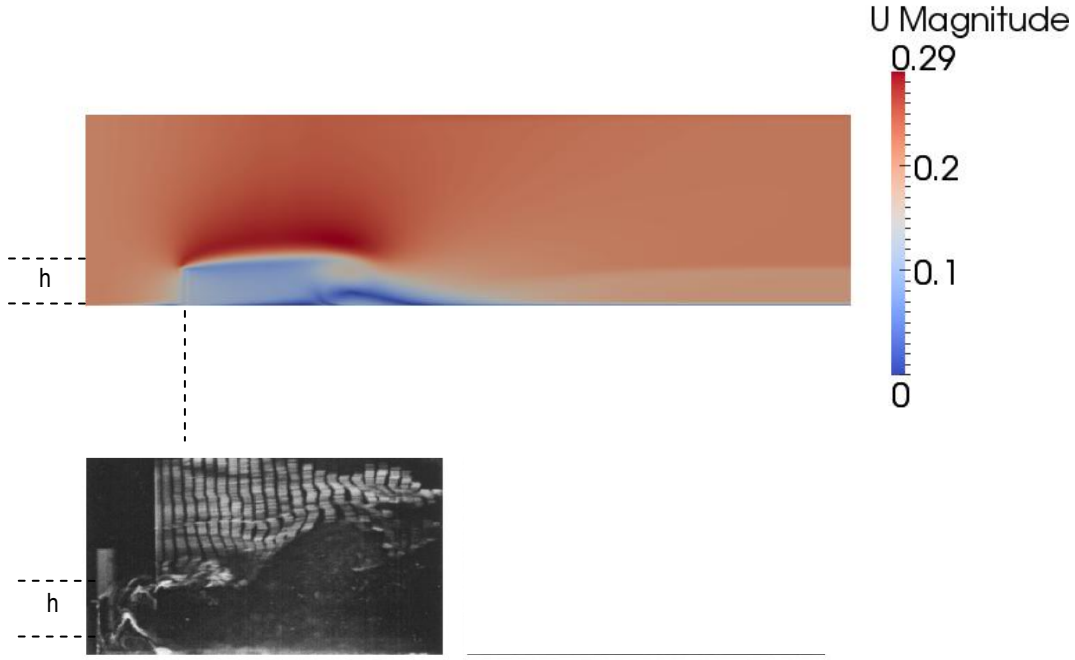

Figure 8 Velocity CFD contour plot compared to Experimental PTV plots for 40% porosity

In order to quantify the flow behviour after the fences the CFD data was sampled using the *sample* utility as defined in a dictionary, *sampleDict*. This indicated the data was sampled for all cells in a vertical line at different multiples of the fence height behind the feature. The first of the four data requests in this dictionary is displayed below as **figure 9**

```
sets
(
   "0.5"
   {
        type    midPoint;
        axis    y;
        start   ( 0.124 0 0 );
        end     ( 0.124 0.2 0 );
        nPoints 100;
   }
```

Figure 9 setFieldsDict entry

Figures 10 and **11** show how the *porousSimpleFoam* model corresponds with experimental data, where **figure 10** is taken from the experimental work and has been replicated well using CFD shown in **figure 11**.

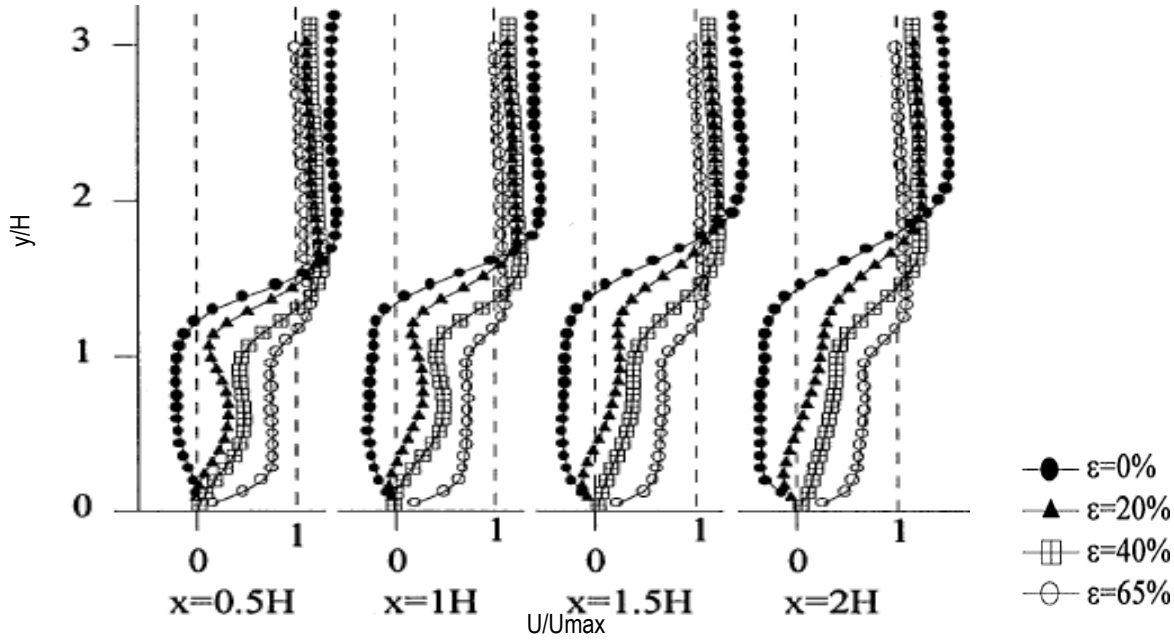

Figure 10 Normalised velocity plots (Lee and Kim 1999)

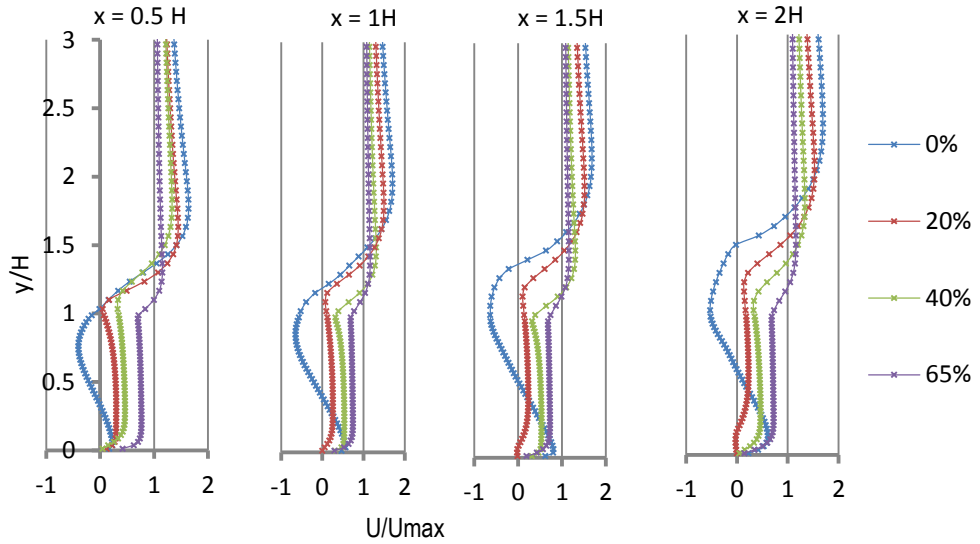

Figure 11 Normalised Velocity Plots 2D PorousSimpleFoam model

Good agreement is shown at the top of the porous region at 0.5 H beyond the fence, where the flow velocity is close to zero for the 0% fence. Increasing the pore volume allows some flow through the fence, with the subsequent flow region tending towards the free stream velocity for the larger the holes in the fence. Additionally, the height at which the flow returns to the free stream velocity increases with distance from the fence to about twice the fence height the in both experimental and CFD datasets.

Discrepancies arise at the bottom of the fence for the lower porosity trials, particularly in the 1.5 H and 2 H graphs for 0% porosity. In these cases, a positive velocity is present up to the height of 0.5 y/H. Conversely, the experimental data shows a negative velocity in this region as would be expected for a wall with no pores.

It is likely that this is caused by poor modelling of the recirculation zone behind the fence due to the k-ε model. Nevertheless, since this study has demonstrated good agreement with the velocity profiles, it is inferred that the Darcy Forchheimer pressure drop within the

porousSimpleFoam model is a reliable method for modelling the flow behaviour with some small errors. As stated above, turbulent effects are not relevant with the laminar flow in this region and therefore any discrepancies should not affect the models in this investigation.

4.3.4 Comparison of the *porousSimpleFoam* model to micro CFD and ALM methods

Although the results shown in **section 4.3.3** demonstrated that the flow through the porous zone in *OpenFOAM* can accurately model experiential data, it was instructive to use this method to compare the investigations of J. Please and A. Begley.

The micro model and up-scaled ALM method used for the equivalent experimental sections of the group work were compared for a range of particle Reynolds numbers in order to establish a validated computational method for specifying the soil permeability. This work demonstrated that it is not reasonable to consider soil to be acting as a packed bed (Please 2012). This was corroborated by the work of others (Baker, Young and Tabor 2011) (Baker and Tabor 2010) where a packed bed of cylinders did not fit the expected trends as well as a packed bed of spheres. It was therefore decided to compare the data with pressure drop per unit length as a function of velocity.

In order to demonstrate that the macro porous model developed for this project performs in a similar manner to the experimental data a small model was constructed to demonstrate the validity of **equations 12** and **13**. The resulting trends add further weight to the conclusions on the validity of the CFD model**.**

This simple model was constructed as a single block, 0.1 m in height to mirror the ALM model. The structure was defined as a cylinder in *blockMesh* by specifying edges that went through points on a circle. The resultant model is shown in **figure 12** next to the ALM model it replicates.

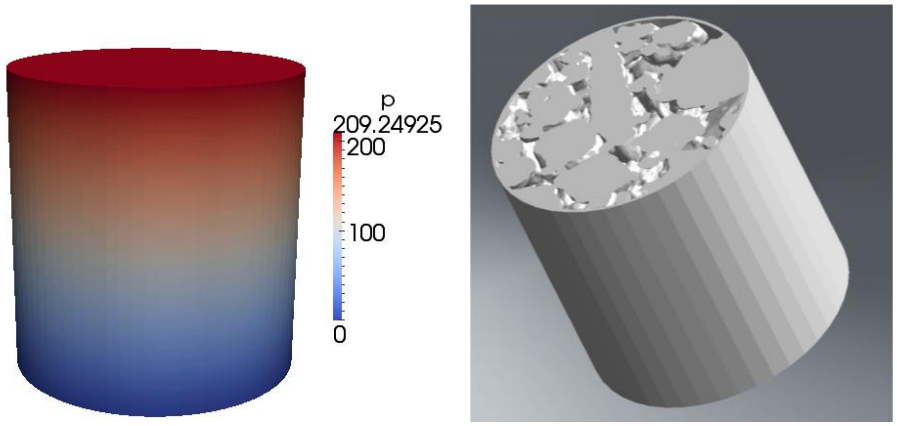

Figure 12 PorousSimpleFoam model of ALM experimental sample (Please 2012)

Coefficients D and F were calculated using the average particle diameter, d_{50}. This value is a weighted average based on the sieve tests conducted as part of the soil structure analysis conducted for the experimental phases of the project (Please 2012). This yielded a value of 2.3 mm taken as a median value from the soil sampled from the case study. This was scaled-up to 17.9 mm to match the ALM model.

The void fraction was calculated directly from the models taken from the *ScanIP* meshes produced for the micro elements of the project (Begley 2012) as 0.2497. These two geometries produced the following coefficients for the porous zones.

$$D = \frac{150\ (1 - 0.2497)^2}{0.0179\ \times 0.2497^3} = 1.7 \times 10^7$$

$$F = \frac{3.5(1 - 0.2497)}{0.0179\ \times 0.2497^2} = 9.45 \times 10^3$$

This model was run, producing the trend added to the graph shown as **figure 13** (Please 2012) labelled as 'Homogenous model'. This trend produces three times the pressure drop compared to the experimental data although this did match the Ergun trend which was specified using the same values. It was deemed that the micro CFD did fit the expected trends although the absolute values were invalidated (Begley 2012).

To this end analysis was conducted to determine a margin of error in the sieve tests, but discussions with Professor Javadi suggested that quantifying errors in this sort of test is problematic (Javadi 2012). The <2% loss of material associated with this method yielded errors of only ±0.1 mm which does not account for the discrepancy. It was also deemed that the computer model which was used to create the ALM model output the geometry to an accuracy greater than ±0.1 mm which is the accuracy of the ALM machine given that the model was up-scaled by 7.8 times for the experimental rig.

Without being able to further analyse the errors, an empirical approach was used to assess the level of inaccuracy in the selection of the porous coefficients. A reasonable fit to the experimental data was achieved with a value of 0.368 mm for the scaled-down average particle diameter. This is similar to the 0.36 mm value found from the sieve analysis for the soil sample supplied from *Hydro International (UK)*. Although not from the case study, it is within expected ranges and represents a reasonable departure from the sieve tests for the case study.

Since the micro CFD to experimental comparison demonstrated that the filter media cannot be considered as a packed bed, it is likely that a better method for finding the average particle diameter for the porous zones coefficients is required. However, in the absence of a coherent method found in the body of scientific work considered in **section 2** the best approach was the fit the data iteratively.

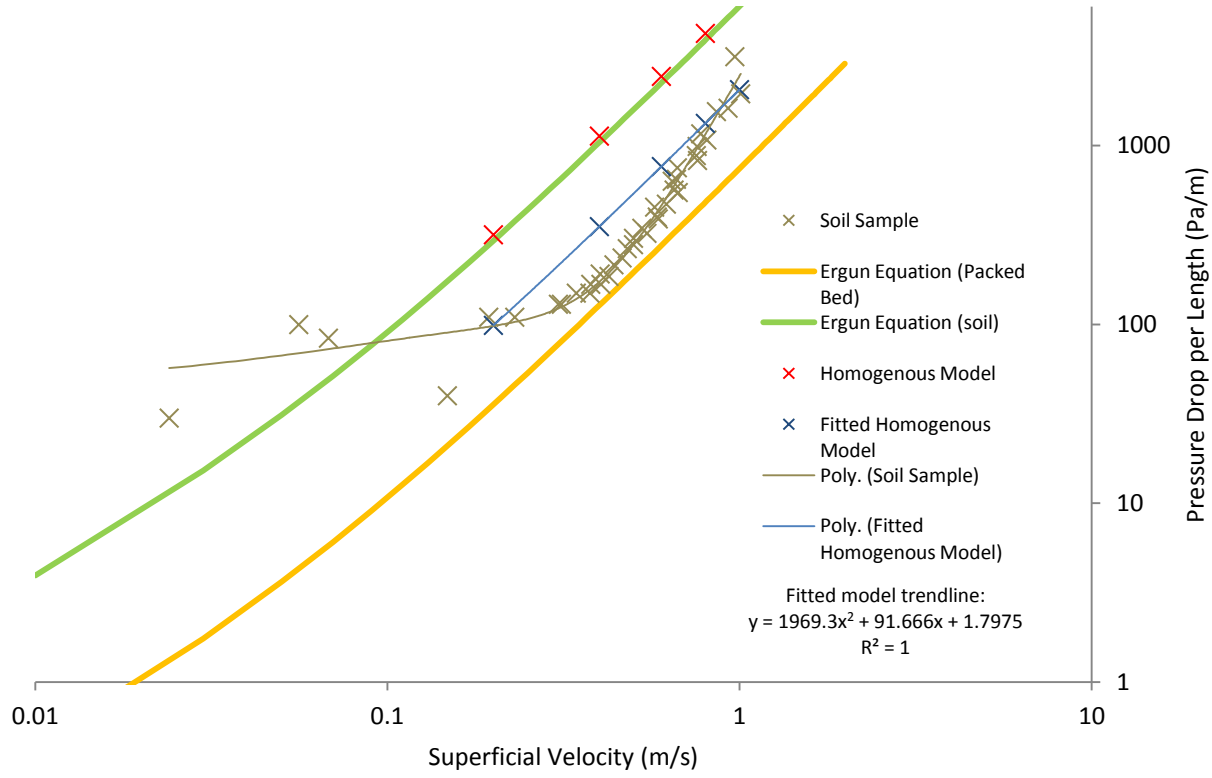

Figure 13 Comparison of experimental and macro porous region tests

The resulting trends of both the 'Homogenous Model' and the fitted curve display the expected quadratic response as they exactly fit second order polynomial curves. This produced a reasonable likeness to the experimental trends. **Figure 13** also shows how the experimental data fits between the Ergun equations trends for both the packed bed and the soil sample. The spread of the lower ALM values was attributed to experimental inaccuracies.

This exercise was valuable in demonstrating the performance of the solver over a range of velocities and showing how close to experimental trends the porous region behaves. This highlighted the need for fitting such values to experimental data rather than using the median particle sizes. Nevertheless, over the valid range of points where experimental errors became acceptable, the trends produced by this second order global method are satisfactory.

4.4 *PorousInterFoam* Validation

4.4.1 *PorousInterFOAM* program outline

There are two fundamental approaches within CFD: Eulerian methods calculate the flow based on a fixed location where as a lagrangian approach calculates the parameters along the flow. The solver *porousInterFoam* uses the Eulerian approach for tracking the location of a free surface through the filter media and is a transient solver as opposed to the steady state operation of *porousSimpleFoam*.

PorousInterFoam tracks the location of the free surface on the model directly in the CFD algorithm. The solution of the governing equations in this case tracks the location of the surface in relation to the surrounding geometry, based on the effects of the walls and filter media.

This is achieved by setting an initial fluid region specified as α_1=1 for liquid before the two phase algorithm is run. The solver then computes the VOF calculation, for each iteration based on a specie transport equation. At any given cell element the VOF is calculated and a weighted average of the physical properties is provided. Thus there is a graded region between the two fluids within which the free surface exists, although its exact location is not specified (OpenFOAM User Documentation 2010).

4.4.2 Research basis

The relevant study described briefly in **section 2.2.1** (Herreros, Mabssout and Pastor 2006) uses a similar level-set approach to *interFoam*. This paper models multiple cases of porous media which includes multiple region models, all compared with VOF multi-phase approaches.

In particular, a hydrostatically saturated vertical column with an air inlet at the top surface and an outlet condition down the left hand side is modelled for comparison. This agrees well with theoretical seepage rates. The porosity of the material is taken as 0.3 and the hydraulic conductivity is considered to be the same for water and air.

4.4.4 Model Construction

The geometry was replicated in *blockMesh*, as a 10.1 x 5 m dam in two dimensions. The water and air viscosities are specified in the *transportPorperties* file, with the original location of the water defined by a maxima and minima vertex in the *setFieldsDict* which specifies the region for the *setFields* utility, run before the *porousInterFoam* solver.

The */0/alpha1* file specifies the boundaries for the indicator function. In this report all studies were constructed with 1 indicating water (red) and 0 as air (blue). Gravity was specified in the */constant/g* file and the geometry constructed to exactly mirror that from the study.

The challenge in the construction of this model was in specifying the correct boundary conditions. Initially, setting the *alpha1* top surface inlet boundary condition to 'fixed value (0 0 0)' displayed significant instability. This was only solved using a function at the inlet, utilising the *groovyBC* code. By specifying a small inlet of water at the left side of the surface, the calculation was stabilised.

The coefficients D and F were calculated in this case using **equations 19** and **20** since there was no geometrical properties specified in the report and this approach does not require the use of an average particle diameter. The values are shown using water fluid parameters.

$$D = \frac{3 \times 1000}{8 \times 1.307 \times 10^{-6}}\left(\frac{1}{0.3^2} - 1\right) = 1 \times 10^{11}$$

$$C2\ (F) = \frac{1}{0.98^2 \times 10.1}(0.3^2 - 1) = 5 \times 10^5$$

4.4.5 Results and discussion

Demonstration of the correct flow patters which are used to demonstrate the validity of this mode can be seen in **figure 14**, showing water seeping out of the vertical dam.

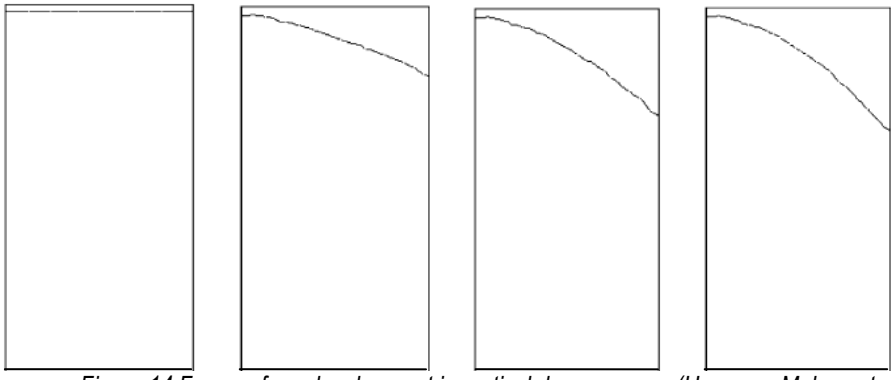

Figure 14 Free surface development in vertical dam seepage (Herreros, Mabssout and Pastor 2006)

As the calculation advances the free surface falls on the right hand side of the model with a curved flow surface developing as the problem evolves from left to right. The *OpenFOAM* model results are shown in **figure 15** where red represents water. The figure displays the position of the free surface at time-steps 0.1 to 0.5 s in 0.1 s intervals.

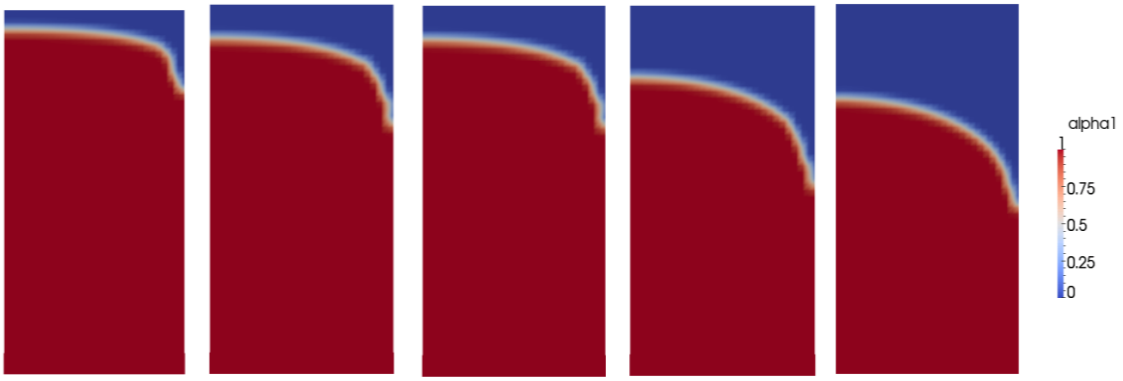

Figure 15 Free surface development in OpenFOAM model

The model shows good agreement with the study in this case. Initially there is a greater drop in fluid level at the outlet face, however this balances out in the later timesteps. Additionally, the height of water on the left hand wall also falls at a greater rate within the CFD. However it is likely that the *interFoam* algorithm is modelling the system more accurately in this case, since this level would also be expected to fall. The 1800 uniform hex cells provide sufficient mesh density to resolve the problem with a thin graded region which adequtely represents the fluid interface.

In general this simple exersise demonstrates the functionality of this solver through fair agreement with free surface patterns, since exact comparisons are a significant challenge to quantify. In order to establish that this behaviour was symtomatic of porous resistance the flow, the patterns were compared for the same region with the porous coefficients set to zero. This displayed a more linear free surface distribution under gravity seepage as shown in **figure 16**.

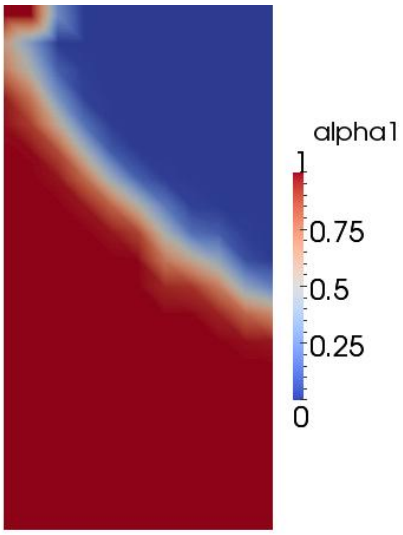

Figure 16 Performance without porousZones specified

4.5 Outflow Mesh Study

4.5.1 Problem Description

The outflow from the *Hydro Filterra*$^{(TM)}$ system comprises a perforated pipe with a solid access section which extends above the soil surface. The outlet pipe sits in 200 mm of gravel and there is 550 mm of filter media soil above as shown in **figure 17**. The mulch layer is ignored for this model.

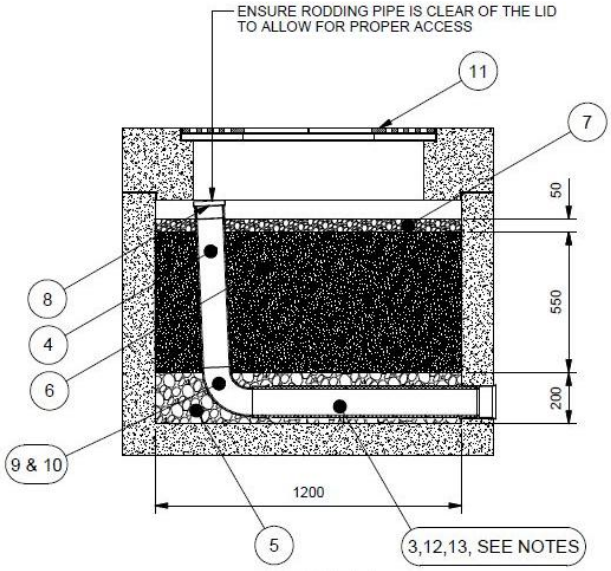

Figure 17. Extract from general arrangement showing pipe configuration and dimensions (Hydro International 2011)

The amount of soil required in the units is calculated by empirical tests and standards. Hence the square cross section of the casing is designed for simplicity rather than as a result of flow-based design intent. Internal imaging techniques such as PIV and PTV depend on the tracking of particles in the flow. This is problematic within a particulate porous medium and therefore there is no way of experimentally visualising the flow within the porous region to inform the design.

However, as the validation exercises demonstrate, computational methods can indicate the flow patterns within the soil and highlight areas for further study. Therefore an investigation was conducted to determine the best approach for modelling the flow inside the *Hydro Filterra*$^{(TM)}$ unit, with care taken to correctly incorporate the outlet pipe into the model.

The information gleaned from the studies into multi-phase flow indicates that there are significant instabilities associated with the flow of a denser fluid into a less dense fluid region as with seepage. Therefore a study was conducted into three meshing approaches which used three different meshing software packages: *ANSYS FLUENT* 12.0, the *snappyHexMesh* utility within *OpenFOAM* and *Pointwise*. This not only produced different quality meshes to assess the simulation under different meshing configurations, but also serves as an application-specific investigation which indicates to *Hydro International (UK)* which software is most suited for modelling this system.

4.5.2 ANSYS Construction

Unlike the open-source software *OpenFOAM*, the *ANSYS FLUENT* CFD code is a closed-source package. What it loses in user control it gains in ease of use through the Graphical User Interface (GUI). Additionally, the large cross-software compatibility within *ANSYS workbench* links mesh generation to CAD software through to the solver and post processing stages in one umbrella program. In this case the model was constructed using *SolidWorks* and imported into the workbench for mesh refinement.

The refinement was applied using the 'refinement centre' global definition. This allowed the tetrahedrons to be automatically generated, and also giving scope for surface-proximity refinement. Three meshes were generated for the soil and gravel regions using coarse, medium and fine refinement options and exported as ascii *.msh* files. These were imported into *OpenFOAM* within the root of the case folder and the relevant mesh files converted into an *OpenFOAM* mesh in the folder */constant/polyMesh* by using *fluentMeshToFoam* utility.

Care was taken at this stage to designate the boundaries of the mesh in accordance to the boundary files already established in the *OpenFOAM* model. It was noted that multiple boundaries can be specified within the same model and this information is retained during the conversion. Methods for specifying the two porous zones within this package were investigated. However, there were difficulties encountered in over-defining internal walls and the zones were specified within *OpenFOAM* after mesh conversion.

In order to model multiple zones, the dictionary *topoSetsDict* was used to specify two labelled regions between maxima and minima vertices. All the cells within the specified regions are then defined as a cell 'set' with the *topoSet* utility. These sets are then defined as cell zones by use of the *setsToZones* command. This writes these cell sets to zones specified in the dictionary, and in this case, they correspond to the 'soil' and 'gravel' of the *porousZones* file. These can be viewed separately in *paraView* and are shown below in **figure 18.**

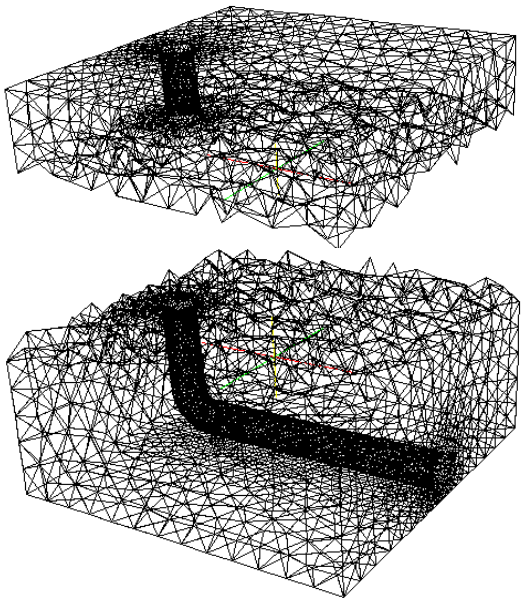

Figure 18 Separated zones in example coarse ANSYS mesh

The system was simulated using very simple boundary conditions. Since the inlet was studied by others (Tarrant 2012), the worst case flow of an influx of a large body of water was simulated using a initially set-field in the top of the model, 0.1 m thick. This also simplified the inlet condition within the */0/alpha1* file as no *groovyBC* case was required as in **section 4.3.4**.

A representative inlet velocity of 1m/s was specified at the top surface. The walls were set with no pressure gradient and zero velocity. Only the horizontal section of the pipe was modelled as an outlet by specifying the appropriate *inletOutlet* condition. The system was designed to allow for a variable time-step within the *controlDict,* to maintain the couront number below 0.2 to adjust for instabilities.

4.5.3 ANSYS Mesh Results

The resulting flow pattern for the coarse mesh is shown below as **figure 19** which shows the body of the mesh as a wireframe with a clip at the pipe cross section. As before, the indicator function alpha1=1 represents water and blue represents air in the unsaturated media. **Figure 20** shows the evolution of the free surface as the simulation progressed.

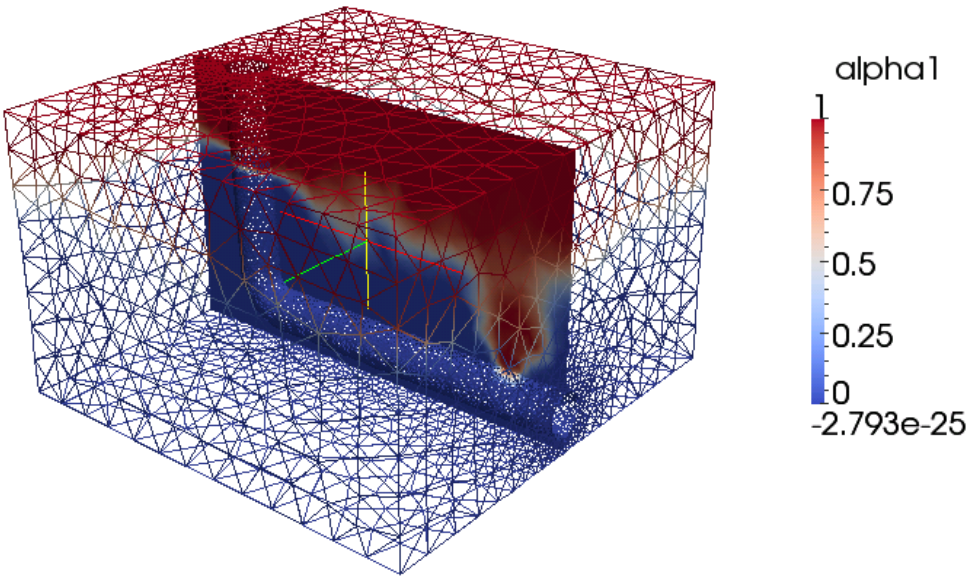

Figure 19 Coarse ANSYS mesh alpha1 plot

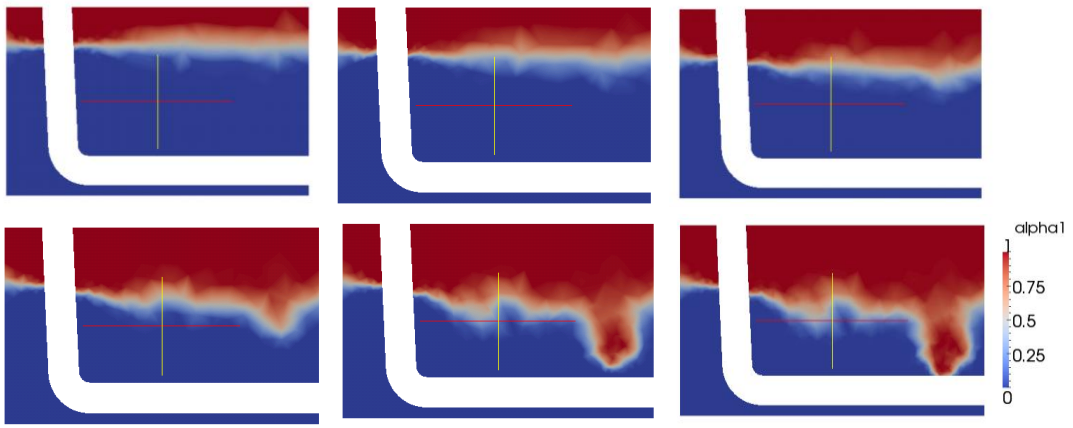

Figure 20 Evolution of free surface in coarse ANSYS mesh in order 0, 0.03, 0.0643, 0.098, 0.123 and 0.127 s

The system failed after 489 iterations at a simulation time of 0.127 s due to a numerical instability (floating point exception). It can be seen that the coarsest region of the mesh, at the free surface furthest from the pipe, was the location where the first downward flow of water developed.

It is not surprising that the system produced a flow 'finger' at the largest and lowest of these mesh elements near the initial free surface. As the flow progressed in this region, a set of equivalent upward air 'fingers' developed. Although it is not possible to visualise all of these features in a 2D clip, one such vertical air 'finger' can be seen developing to the left of the main water finger in each image.

This behaviour is a physical phenomenon which introduces a numerical problem; the Rayleigh Taylor instability highlighted in the literature review. This instability is triggered as the 'fingers' develop at the non-uniform elements in the mesh. The fact that this is triggered by mesh quality was demonstrated by running the same size domain with a uniform hex mesh created in *blockMesh* without any pipe detail. The results, shown in **figure 21**, demonstrate that the expected pressure drop was exhibited as the flow progressed successfully from top to bottom with no 'fingers' developing.

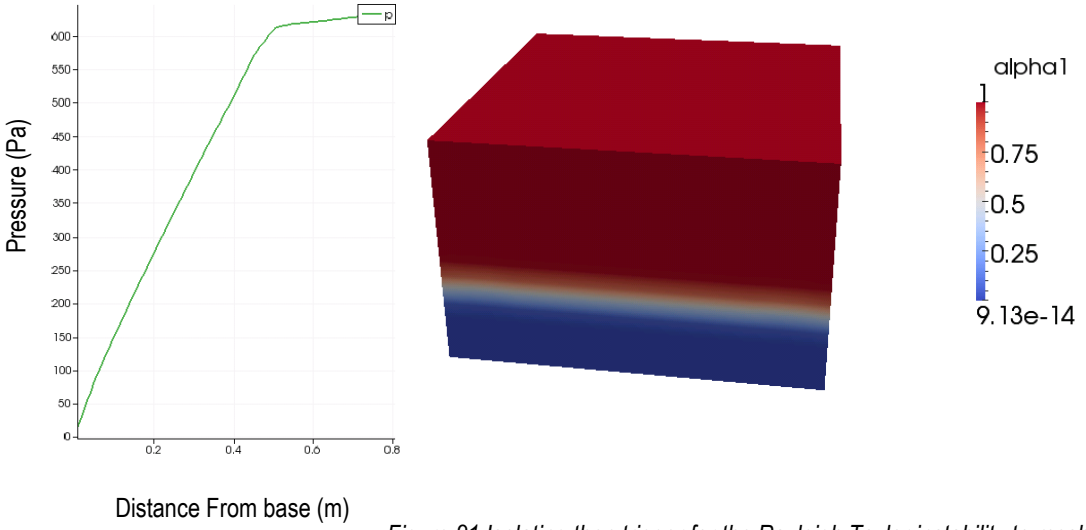

Figure 21 Isolating then trigger for the Rayleigh Taylor instability to mesh quality

To investigate the limits of the *porousInterFoam* solver to deal with this problem, two finer meshes of the unit were produced in the same way and were run using the same conditions. This was intended to reduce numerical errors produced from any poor mesh elements and isolate the problem to the recognised physically-derived instability. The next finest refinement produced the 'fingering' effects shown in **figure 22** similar to those sourced from other work.

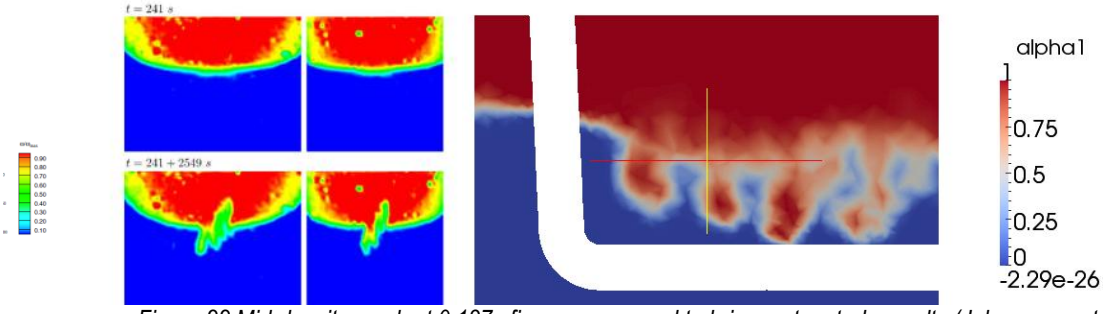

Figure 22 Mid-density mesh at 0.137s fingers compared to brine-water study results (Johannsen, et al. 2006)

In this case more than one principle 'finger' developed in the flow, demonstrating how a finer mesh does not necessarily solve this instability. Rather, the reduced element sizes mean that more than one 'finger' develops and the simulation failed in this case at a similar point.

Further refinement of the mesh demonstrated how the instability can cause the system to fail based on only the earliest onset of 'fingering' as can be seen for the finest *ANSYS* mesh in **figure 23**. Although the presence of flow 'fingers' is not obvious, the previous trends suggest that in this case the mesh is creating multiple miniature 'fingers' and is failing as a result.

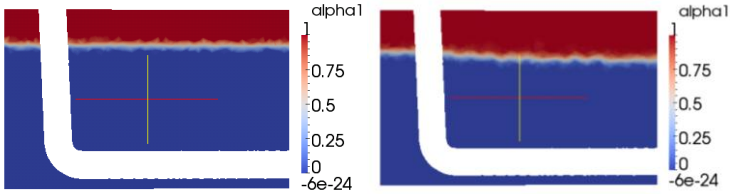

Figure 23 Failure of finest ANSYS mesh after only 3 recorded time-steps

4.5.4 SnappyHexMesh approach

SnappyHexMesh takes a uniform region generated through *blockMesh* and begins a three step meshing process where the quality of the final mesh is controlled by a *snappyHexMeshDict* file. The first entries in this dictionary switch on the three steps to the process: castellated refinement, snapping and adding layers. The code identifies the feature geometry by file name so that *snappyHexMesh* can search the constant/*trisurface* folder for the 3D model in the form of .stl data. The three mesh processes are written to time-step style files inside the case file labelled 0 to 3.

Three separate meshes were created using this utility with increasing levels of refinement at the pipe surface. The initial mesh was created using *blockMesh*. This method utilises the original cell zones which are retained after the *snappyHexMesh* refinement has been completed. The resulting coarse mesh is shown below as **figure 24** which specified between three and four refinement levels. These can be clearly identified by inspection where the outlet section of the pipe joins the far wall. .

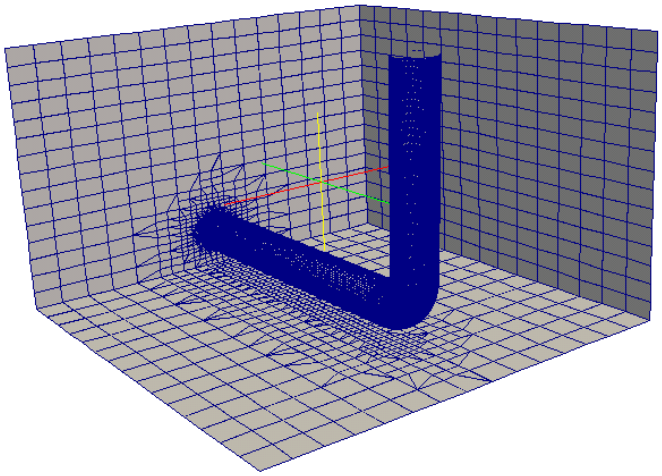

Figure 24 Mesh created with snappyHexMesh

It was expected that due to the uniform nature of the mesh in the majority of the domain this simulation would be more stable than the *ANSYS* methods described in **section 4.5.3**. However none of the three meshes solved enough timesteps to yield any change in free surface location. *CheckMesh* was run on each mesh to assess the mesh quality in each case but no highly skewed faces or non-orthogonal cells were identified. In an attempt to stabilise the solution upwind differencing was selected on all available differencing schemes within */system/fvSchemes* although this did not yield any significant changes.

It is noted that the best results were achieved with coarse, uniform meshes within the *ANSYS* study. Therefore the instability is not necessarily associated with a poor mesh quality but perhaps a sudden significant change in mesh density as exhibited with *snappyHexMesh*. Hence it is recognised that uniformity in the mesh may be significant.

4.5.6 *Pointwise* Construction

To further investigate this effect, another possible mesh construction package, *Pointwise* was utilised. The basic functionality of this software constructs meshes using a linear approach. Previous methods involved building a domain within which the mesh is defined, as with the *blockMesh* to *snappyHexMesh* or within the *SolidWorks* to *ANSYS* processes described above. Rather for *Pointwise,* individual sides are defined with a number of elements and extruded to

create 'domains' or faces which define the number of elements that are then automatically populated within the region.

A surface and line file of the geometry was imported in .iges format. The lines were used to specify a set of faces with a defined tetrahedral mesh density and the domain was then automatically populated without surface refinement to ensure a uniform region as shown in **figure 25.** Although the mesh is coarse it can be seen from this figure that good uniformity been achieved.

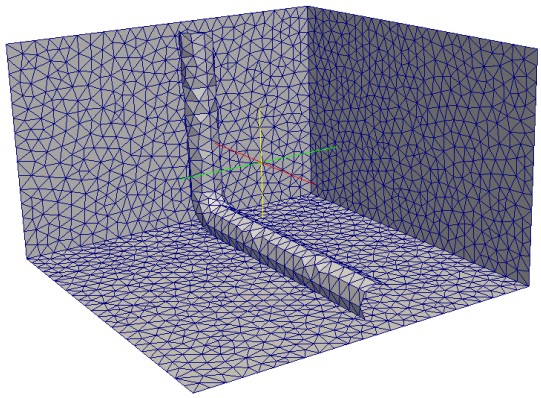

Fig 25 Uniform Pointwise Mesh

Further advantages of this package compared to *ANSYS* includes the export format which can directly write the relevant *constant/polyMesh* files required for *OpenFOAM* without requiring the use of other utilities. With this approach the boundary patches can also be defined within the meshing software.

4.5.7 *Pointwise* Results

The results of the simulation using the conditions described in **section 4.5.2** with the uniform *Pointwise* mesh, do not display the same behaviour as the *ANSYS* approach. A high number of iterations were computed, allowing the flow to seep towards the pipe. The wire-mesh plot is shown as **figure 26** with the evolution of the flow surface in the central plane shown as **figure 27**. Alpha1 respects the same conventions in previous sections.

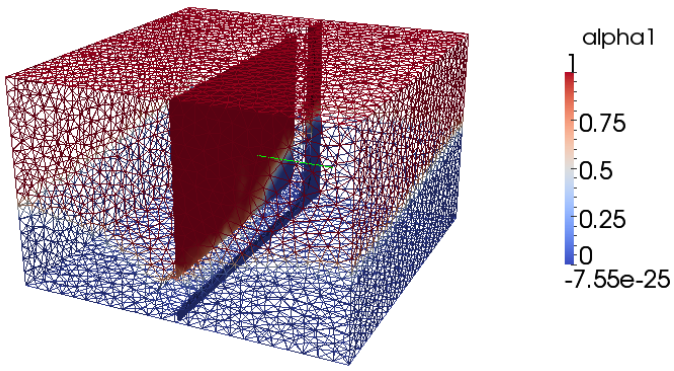

Figure 26 Flow Patterns in wire mesh constructed in Pointwise

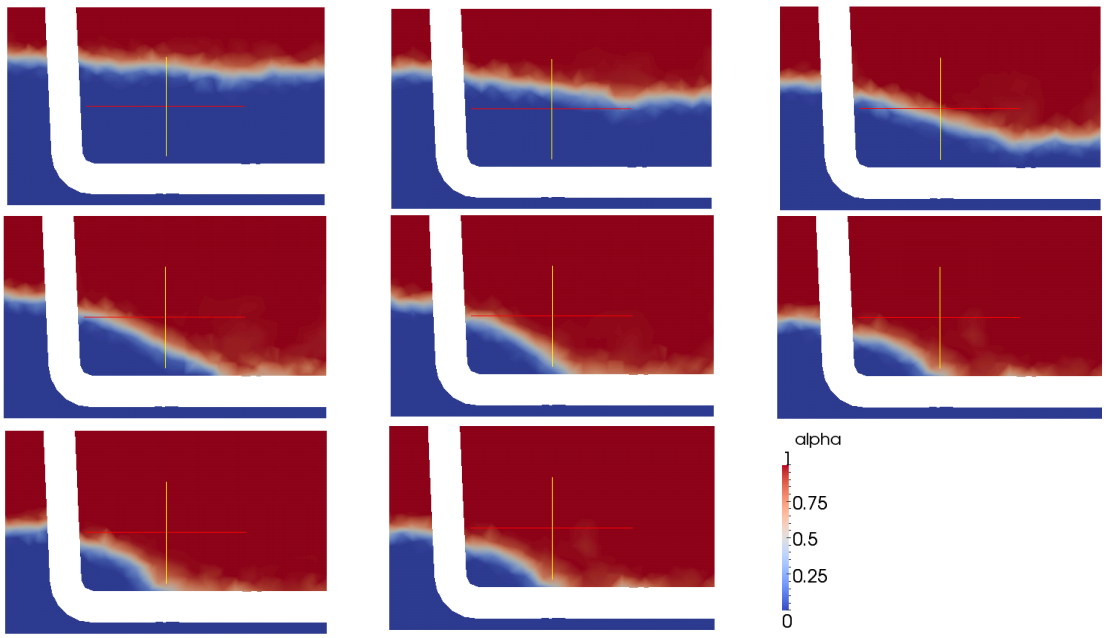

Figure 27 Evolution of free surface in the Pointwise mesh time steps 0.11,0.25,0.182,0.216,0.311,0.356,0.0588,0.3558 s respectively

Although tentative, the validation of the porous models and the absence of significant instability in this model indicate that this has resolved the system more successfully than previous models and some tentative conclusions can be drawn from this study.

It is noted how the flow at the walls significantly effects the free surface pattern. Without the onset of 'fingering', the flow near the rear wall is significantly retarded as in the *ANSYS* models, but in this case, without the instability featuring to such a high degree, a similar trend is displayed at the side walls. The majority of the seepage occurred within the central region, directly above the pipe.

This is possibly caused by the retarding effects of the walls. However the lack of this behaviour at the end opposite to the vertical pipe section indicates that it is more likely the presence of the pipe allowing the air to escape which is accelerating the flow above the outlet, as seen clearly in **figure 28.**

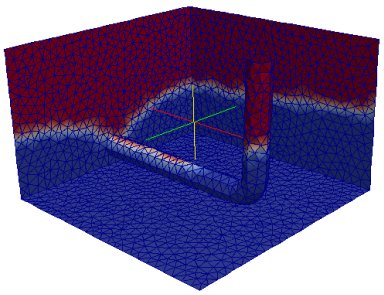

Figure 28 Central flow area and wall effects

This pattern indicates that the flow introduced to the pipe may create stagnant regions at the bottom edges of the unit. Since these areas do not efficiently use the filter media material economies could be achieved by constructing two inclines at the base meeting in the middle. Such a 'v' shaped design could save filter media, reducing material costs without significantly effecting retention times. However this concept would require further study.

4.5.8 Porous Baffle

The outlet pipe was modelled using a simple outlet condition without any porous jump although the perforated design could be modelled as a porous region. Little information was known about the nature of this feature since it is simply described in the general arrangement as a perforated pipe section.

It is possible to model this feature using a porous baffle, specifying a change in pressure across the boundary between cells. However in this case, it was deemed beyond the scope of the meshing study and the numerical instabilities and mesh uniformity issues were considered more significant issues to consider. Therefore the application of this method could form an area of further study.

4.5.9 Recommendations

Three general recommendations for further work arise from this study: Firstly the best software and mesh approach used are highlighted, possible design concepts arising from the current models are outlined and finally, potential advances in the computational modelling techniques are discussed.

The meshing approaches were compared using a matrix analysis. The licence costs, compatibility, ease of use and versatility as they pertain to this application were rated out of five with reasons given. These values were then weighted giving greater value to the licence cost considerations and least to versatility. The results are shown in **table 2.**

Table 2: Matrix Analysis

	Licence estimates			Compatibility			Ease of use			Versatility			
Weighting:	7			4			6			3			
Method	**Detail**	**Value**	**Weighted**	**Detail**	**Value**	**Weighted**	**Detail**	**Value**	**Weighted**	**Detail**	**Value**	**Weighted**	**Total (%)**
ANSYS	£10K	1	7	SolidWorks	3	12	Satisfactory GUI	3	18	Comprehensive	5	15	**52**
SHM	Open-source	5	35	through .stl	2	8	C++ competency	2	12	Limited refinement method	2	6	**61**
Pointwise	£6K	2	14	All methods	5	20	Intuitive GUI	4	24	Comprehensive	5	15	**73**

With a rating of 73% *Pointwise* was deemed the best approach for this application since the meshes produced are most appropriate for this construction. Additional benefits such as the vast compatibility of this package are also likely to justify the licence cost. The poor mesh uniformity of *snappyHexMesh* methods mean that, in this application, it was not deemed the best approach. This package is already in common use at *Hydro International (UK)* for other meshing operations. However, only a single *Pointwise* licence would be required for this recommendation so that appropriate meshes for multi-phase applications could be constructed.

5. Collaborative work: Construction of the large-scale 3D Model

5.1 Overview

This section describes the work undertaken to combine the efforts of the three macro-scale CFD elements of this project. The other sections are summarised here to highlight the lessons used in the collaborative section. The combined work completed is then described, outlining the model construction and fault finding approaches undertaken.

5.1.1 Summary of Roots Study

The study of the root system (Ronald 2012) involved a comprehensive study of flow in porous media which is populated by root structures. The micro-scale studies involved taking micro-CT scanned samples and identifying an approach for correctly specifying the flow through the branches. An image of the model is shown on the left in **figure 29.**

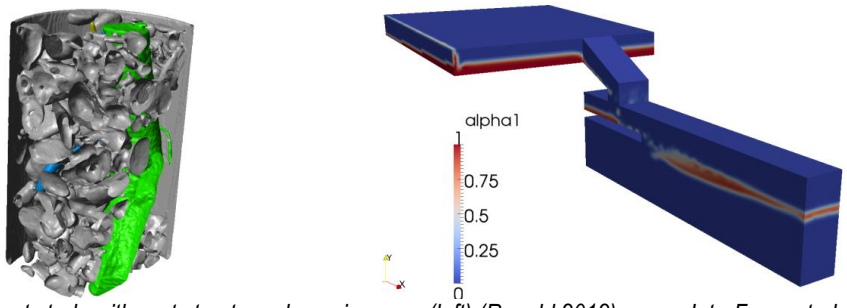

Figure 29. Micro root study with root structure shown in green (left) (Ronald 2012) porousInterFoam study of inlet condition (right) (Tarrant 2012)

Scaling this up to a macro-level involved creating a representative fractal root structure and meshing this using *snappyHexMesh*. Investigations using *porousSimpleFoam* utilised the methods identified by this section to specify the porous zones and changes in the flow patterns were identified.

5.1.2 Summary of Inflow Condition

The inlet from the ground surface to the *Hydro Filterra*$^{(TM)}$ unit (Tarrant 2012) involved comprehensive use of the *blockMesh* feature to construct geometries which represent the system. Application of the porous zone methods identified in this section, led to an instructive study of the inlet conditions. The absence of the Raleigh Taylor instability within these models is of particular interest to this study. It is likely that since the inflow can be seen at a discrete location from the energy dissipating stones, the model was solvable although there is some dispersal of air within the water represented (right) in **figure 29.**

This work involved a significant effort in mesh generation and specifying the correct boundary conditions including the use of *groovyBC*. Additionally, this report highlighted the value of using the k-ω turbulence model for simulating drainage problems of this nature.

5.2 Model Construction

5.2.1 *SnappyHexMesh* generation of the final result

The 3D model was meshed using *snappyHexMesh*. This method was chosen to allow the model to be compatible with the current resources available to *Hydro International (UK)*, providing scope for future development. This also made it easier to combine the work of all three sections of the macro-level studies since this approach was used for specifying the root mesh. This decision also respected licence availability at the time of mesh construction.

The geometry constructed within *SolidWorks* (Russell 2012) was used to create the casing geometry, including the inlet channels. The road surface and roots were combined with the outlet pipe constructed for this work by J. Ronald as an assembly within *SolidWorks,* yielding ten surface files. This allowed different refinement levels to be specified in separate parts of the mesh. For uniform sections such as the road surface the mesh was refined to a maximum of 3 levels while around the roots, 8 levels of mesh refinement were specified. The resulting mesh is shown as **figure 30.**

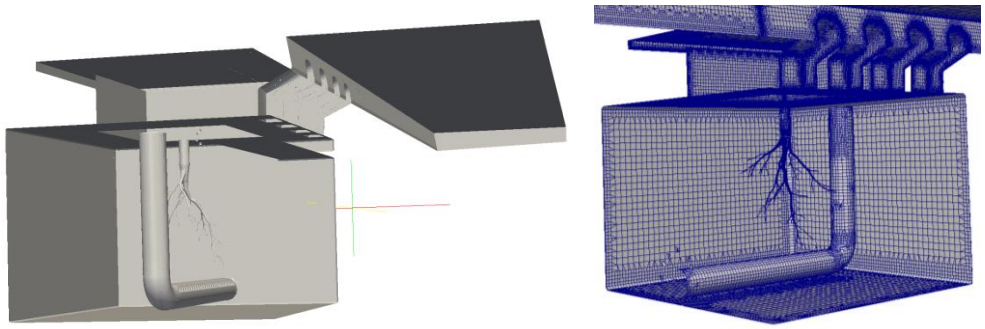

Figure 30. 3D Mesh generated

The porous regions were specified using the zone setting methods outlined in **section 4.5.2** and the Darcy Forchheimer approaches identified above.

5.2.2 Boundary Conditions

The system was initially constructed to simulate a cross channel flow on the road surface, with water-only outlet through the root system and the outflow through the outlet pipe as specified by this project.

The inlet at the far edge of the of the road surface, perpendicular to the kerb was specified using *groovyBC* for half the road domain to be filled with water and the *setFieldsDict* was written accordingly. An extract of this file is shown as **figure 31**.

```
inflow
{
  type            groovyBC;
  variables "surface=0.22;";
  valueExpression "(pos().z<=surface) ? 1.0 : 0.0";
  value           uniform 1;
}
```

Fig 31 Road surface inlet condition (Tarrant 2012)

Prior to this point no work had been completed on multi-phase flow around the root system and so the */0/alpha1* entry was added for this feature to respect the *porousInterFoam* requirements. The relevant water-only outlet condition is shown as **figure 32**

```
{
    type            inletOutlet;
    inletValue      uniform 1;
    value           uniform 1;
}
```

Figure 32. Alpha 1 Outlet condition for the root system

5.2.3 Fault Finding

Although the system geometry was constructed successfully the model could not be solved. This was not surprising since combining such systems cannot be considered a linear approach. The combination of models may introduce instabilities in the calculation that were not present in any of the previous models.

The approach undertaken to solve these issues aimed to isolate the fault in the system. Work was conducted to sequentially demonstrate that the issues highlighted by each macro CFD section of the project were not the cause of the failure. The system was re-meshed without the roots present and the system could not be solved, proving that it was not uniquely associated with *porousInterFoam* around the roots.

Furthermore the system was reconstructed using *porousSimpleFoam* to remove the potential present of Raleigh-Taylor instabilities; however this did not solve the system either. Visualisations of the initial models indicated the mesh was very coarse at the road surface and the total number of elements in the initial *blockMesh* was doubled in each direction to refine the mesh in this location. When this also proved to be unsuccessful, an investigation into refining the mesh at each location was conducted, raising the mesh refinement levels to 10 around the roots and to 7 in other areas. Around 8 different level combinations were tried without resolving the issue, indicating that the error may be a more fundamental issue with the meshing approaches used.

In summary, this analysis suggested that the error was not uniquely based in the *porousInterFoam* application around the roots or the mesh quality at the road surface. Furthermore the failure of the *porousSimpleFoam* model demonstrated that the error was not uniquely found in the Raleigh Taylor instability.

To further this study it would be instructive to construct a *porousInterFoam* model of the flow past the roots to demonstrate that this can be solved. Replication of the inlet study using *snappyHexMesh* should be conducted to demonstrate that the mesh in this region is also solvable. Once these are completed successfully it would be possible to build the model sequentially in order to isolate the problem to the interface between two sub-models if that is the source of the error. A possible further investigation would be to create the geometry using *Pointwise* to create a more uniform mesh.

6. Conclusions and Recommendations

6.1 Summary

The first stage of this project comprised the building of models using the steady state solver *porousSimpleFoam*. A method to specify the porosity of the region based on physical properties of the medium was identified and the results were experimentally verified. Additionally they provided a good fit to experimental trends within this project.

Building on this, the VOF method, *porousInterFoam,* was used to evaluate multi-phase flow within the filter media. For modelling the *Hydro Filterra*$^{(TM)}$ geometry, meshes were generated using three different packages: *ANSYS workbench*, *snappyHexMesh* and *Pointwise*. These were compared, determining that the use of *Pointwise* minimised model instabilities for storm surge flow into unsaturated media.

Extending this work and collaborating with the other macro-level studies within this project, the large-scale 3D model was constructed with inlet, porous media, roots and outlet conditions respected. This was constructed using *snappyHexMesh* for compatibility with the other studies and due to resource availability. Despite multiple attempts at applying different boundary conditions and mesh refinement levels, the system could not be solved.

The most significant conclusion arising from this study is that the uniformity of the mesh within the porous region is vital for resolving a multi-phase system under surge conditions. Additionally the methods identified within this work demonstrate a good fit to experimental data. These can serve to construct instructive models with homogenous porous regions which can be useful for broad design decisions. This is achievable provided that the porous resistance values used are specified in comparison with experimental data to specify the system correctly rather than using theoretical approaches.

6.2 Identifying areas for Further Development

Extension of this project could include the introduction of a saturation-dependant porous resistance. This would require editing the source code to allow fluid-dependant porosity and would allow the use of the relative permeability methods for *porousInterFoam* simulations.

To complete the 3D model, improvement and modification of mesh quality is needed, particularly in regard to mesh uniformity. Whilst the individual elements of the system have been accurately modelled, the mesh refinement required to create an adequately uniform combined geometry would necessitate additional time and resources.

6.3 Recommendations

This work has been valuable in identifying and validating a method for specifying the porous regions within the *Hydro Filterra*$^{(TM)}$ unit. The work completed in this section of the group project demonstrates the need for uniformity of meshes and therefore recommends that further study is conducted using models created within the meshing package, *Pointwise*. The models created with this method indicated that there is scope in refining the casing design through a 'v'-shaped base to save on filter material, making the design more sustainable. As demonstrated in this study it is through such computational approaches that flows in opaque filter media can be characterised to inform design decisions.

References

ANSYS Inc. *ANSYS FLUENT 12.0 User Manual: 7.2.3 Porous Media Conditions.* 29 01 2009. www.sharcnet.ca/Software/Fluent12/html/ug/node233.htm (accessed 03 05, 2012).

Atta, Arnab, Shantanu Roy, and K.D.P. Nigam. "Prediction of pressure drop and liquid holdup in trickle bed reactor using." *Chemical Engineering Science 62*, 2007: 5870 – 5879.

Atta, Arnab, Shantanu Roy, and Krishna D.P. Nigam. "Investigation of liquid maldistribution in trickle-bed reactors using porous." *Chemical Engineering Science 62*, 2007: 7033 – 7044.

Baker, M.J., and G.R.Tabor. "Computational analysis of transitional air flow through packed columns of spheres using the finite volume technique." *Computers and Chemical Engineering 34*, 2010: 878–885.

Baker, M.J., P.G. Young, and G.R. Tabor. "Image based meshing of packed beds of cylinders at low aspect ratios using 3d." *Computers and Chemical Engineering 35*, 2011: 1969– 1977.

Bear, Jacob. *Dynamics of fluids in porous media.* New York: American Elsiever, 1972.

Begley, Alastair. *Three Dimensional Image Based Meshing and Computational Analysis of Fluid Flow in Various Porous MediaT.* I2 Group Report, Exeter: Exeter University, 2012.

Berre, Inga, Martha Lien, and Trond Mannseth. "Muti-level parameter structure identification for two-phase porous-media flow problems using flexible represnations." *Advances in Water Resurces 32 issue 12*, 2009: 1777-1788.

Braun, Christopherus, Rainer Helmig, and Sabine Manthey. "Macro-scale effective constitutive relationships for two-phase flow processes in heterogeneous porousmedia with emphasis on the relative permeability–saturation relationship." *Journal of Contaminant Hydrology*, 2006: 47-85.

Caron, Pablo. *SnappyHexMesh - How to set-up to avoid skewfaces?* 01 01 2009. http://www.cfd-online.com/Forums/openfoam/70694-snappyhexmesh-how-set-up-avoid-skewfaces.html (accessed 02 27, 2012).

CFD Online. *Turbulence Intensity.* 03 01 2012. http://www.cfd-online.com/Wiki/Turbulence_intensity (accessed 02 12, 2012).

—. *Use of k-epsilon and k-omega Models.* 28 04 2010. http://www.cfd-online.com/Forums/main/75554-use-k-epsilon-k-omega-models.html (accessed 03 28, 2012).

CFD Computing - Power of Numerical Simulation. *snappyHexMesh.* 01 02 2010. http://cfdcomputing.com/documents/snappyHexMesh.htm (accessed 02 26, 2012).

Corapcioglu, M. Yavuz. *Advances in Porous Media.* Amsterdam: Elsiever Science B.V., 1996.

Crolet, Jean-Marie. *Computational methods for flow and transport in porous media* . Dordrecht: Kluwer Accademic, 2000.

Engineering Toolbox. *Water- Dynamic and Kinematic Viscosity.* 05 01 2010. www.engineeringtoolbox.com/water-dynamic-kinematic-viscosity (accessed 04 19, 2012).

ESI. *esi info.* 2010. http://cms.esi.info/Media/productImages/28683_1313421457846_PF.jpg (accessed 12 2, 2011).

Hafsteinsson, Haukur Elvar. "Porous Media in OpenFOAM." *Chalmers*, 2009: 1-14.

Health and Safety Executive. *Working with VDUs.* Information Leaflet, London: H&S Executive, 2006.

Hendricks, David W. *Fundamentals of Water Treatment Unit Processes.* Boca Raton: CRC Press Taylor and Francis Group, 2011.

Herreros, M.I, M. Mabssout, and M. Pastor. "Application of level-set approach to moving interfaces and free surface problems in flow through porous media." *Computational Methods in Applied Mechanics and Engineering*, 2006: 1-25.

Hydro International. "HF-1200-100." *Filterra(TM) General Assembly.* Cleaveland: Hydro International, 01 01 2011.

Hydro International. *Sizing Guide.* Product Guide, Cleavland: Hydro International, 2010.

Javadi, Akbar, interview by James Please. *Professor* (20 04 2012).

Johannsen, Klaus, Sascha Oswald, Rudolf Held, and Wolfgang Kinzelbach. "Numerical simulation of three-dimensional saltwater-freshwater fingering instabilities observed in a porous medium." *Advances in Water Resources*, 2006: 1690-1704.

Lee, Sang-Joon, and Hyoung-Bum Kim. "Laboratory measurements of velocity and turbulence field behind porous fences." *Journal of Wind Engineering*, 1999: 311-326.

Lopes, Rodrigo J.G., and Rosa M. Quinta-Ferreira. "Turbulence modellingofmultiphaseflowinhigh-pressuretrickle-bedreactors." *Chemical EngineeringScience64*, 2009: 1806--1819.

Ma, Xiang, and Nicholas Zabaras. "A stochastic mixed finite element heterogeneous multiscale method." *Journal of Computational Physics 230*, 2011: 4696–4722.

Macini, P., E. Mesini, and R. Viola. "Laboratory measurements of non-Darcy flow coefficients in natural and artificial unconsolidated porous media." *Journal of Petroleum Science and Engineering 77*, 2011: 365–374.

Maitra, M.K., N.C. Ghose, and M.k. Maitra. *Groundwater management: an application.* New Delhi: APH, 2008.

Narsilio, Guillermo A., Olivier Buzzi, Stephen Fityus, Tae Sup Yun, and David W. Smith. "Upscaling of Navier–Stokes equations in porous media." *Computers and Geotechnics 36*, 2009: 1200–1206.

OpenFOAM Wiki. *Potential Foam.* 24 11 2009. http://openfoamwiki.net/index.php/PotentialFoam (accessed 02 26, 2012).

Pavey, Stephen. *Macro Scale Computational Analysis Including Porous Media and Free Surface Interaction: Individual Report 1.* Master's Submission: Individual Report - I1, Exeter: Exeter University, 2011.

Petrova, Tatiana, Krum Semkov, and Chavdar Dodev. "Mathematical modeling of gas distribution in packed columns." *Chemical Engineering and Processing 42*, 2003: 931/937.

Please, James. *Micro Scale Experimental Investigation to Determine the Hydraulic Properties of the Hydro Filterra(TM) Bioretention System with Comparison to tests on a Rapid-Prototype Sample and Computer Model Based on the Micro-CT Scans.* I2 Submission, Exeter: Exeter University, 2012.

Prodanovic, Masa, and Steve L. Bryant. "A level set method for determining critical curvatures for drainage and imbibtion." *Journal of Colloid and Interface Science*, 2006: 442-458.

Quigley, Marcus, Aaron Poresky, Marc Leisenring, John Lenth, and Rebecca Dugopolski. *Filterra(TM) Bioretention Systems: Technical Basis for High Flow Rate Treatment and Evaluation of Stormwater Quality Performance.* Technical, Ashland: Hydro International, 2010.

Ronald, James. *Computational Modelling Of Plant Root Architecture and Fluid Absorption through Filtration Media Populated By Root Structures.* I2 Submission, Exeter: Exeter University, 2012.

Russell, Suzanne. *Finite Element Analysis and Optimisation Investigation into the Chamber and Protective Grate used as part of the Bioretention system.* I2 Sumbission, Exeter: Exeter University, 2012.

Sáez, A.E., and R.G. Carbonell. "Hydrodynamic parameters for gas–liquid cocurrent flow in packed beds." *A.I.Ch.E. Journal 31*, 1985: 52–62.

Souadnia, A., and M. A. Latifi. "Analysis of two-phase Flow distribution in trickle-bed reactors." *Chemical Engineering Science 56*, 2001: 5977–5985.

Straughan, B. "Structure of the dependence of Darcy and Forchheimer coefficients on porosity." *International Journal of Engineering Science 48* , 2010: 1610–1621.

Tabor, Dr Gavin. *Tutorial Sheet 1.* Tutorial Sheet, Exeter: Exeter University, 2012.

Tabor, Dr Gavin. *Tutorial Sheet 3.* Tutorial Sheet, Exeter: Exeter University, 2012.

Tabor, G., P. A. Belle, P. Safarik, T. Hyhlik, and P. Stuart. *Sumulation of Porous Fences using Fluent.* Draft Journal Report, Exeter: Unpublished, 2004.

Tarrant, Jon. *Macro Scale Computational Analysis of the Hydro Filterra(TM) Stormwater Drainage System in an Industrial Urban Environment.* I2 Submission, Exeter: Universtiy of Exeter, 2012.

Undergraduate *Filterra(TM)* Group. *First Group Report.* University Coursework, Exeter: Exeter University, 2011.